An Experimental Study on Tensile Fracture of Snow*

by

Hideki NARITA
成 田 英 器
The Institute of Low Temperature Science

Received October 1983

Abstract

Experiments were made on fracture of snow under tensile stress in the laboratory and field, as the tensile fracture plays one of the most important roles in the releasing mechanism of a slab avalanche.

First, specimens, in the cylindrical form 5 cm in diameter and 12.5 cm in length, of natural fine-grained old snow were subjected to a uniaxial tensile experiment in the cold laboratory at various temperatures, the snow density ranging from 240～470 kg・m^{-3} and the crosshead's tensile speed ranging from 6.8×10^{-8} ～3.1×10^{-4}m・s^{-1}, which provided the specimens with the average strain rate in the range from 5.5×10^{-7} ～$2.5\times10^{-3}s^{-1}$. Then, the maximum extension attained was 23 %. Also investigated in the experiment was how much the behavior of snow under tensile stress depends on density and temperature.

As the result of the above experiment it was revealed that, when the strain rate was higher, medium and lower, brittle fracture, two modes of ductile fracture and fractureless creep took place respectively. Accordingly, four general types were classified as to the behavior of snow under tensile stress. In the case of ductile fracture, microcracks appeared locally in a band or all over the specimen when the tensile strain amounted to several percent, which was followed by fracture as the percentage increased.

Secondly, conditions under which microcracks grew were investigated, whereby it was found that fracture started with formation of microcracks. Then, using the critical strain, a description was given to the condition under which snow under tensile stress came to fracture.

Thirdly, the fracture condition obtained in the laboratory using small-sized specimens was examined by subjecting a snow cover on a slope in the field to an experiment, with the result supporting the validity of this condition. Finally, a brief rheological interpretation was given to the fracture of snow under tensile stress.

*Contribution No. 2625 from the Institute of Low Temperature Science
北海道大学審査学位論文

Contents

I. Introduction

According to the Classification of Avalanche defined by Japanese Society of Snow and Ice (1964), the avalanche is classified into two general types, i. e., "point released avalanche (avalanche released from a point)" and "zone released avalanche (avalanche released by a zone or slab)", by a difference in mechanism of avalanche releases, apparently by a difference in areal extent of avalanche sources. While the slab avalanche appears as either full-depth or surface avalanche, the point released avalanche appears only as the surface avalanche. Generally speaking, most of large-scale and disastrous avalanches belong to the slab avalanche type ; they break out frequently throughout the snow season (Akitaya 1974, Ikarashi 1979).

A slab avalanche is released instantly by zonal disintegration of a snow slab on a slope. The snow slab can stay stably on the slope against the gravity, being supported by the neighboring snow cover and the bed ground or snow. The boundary of the slab is generally classified into four parts according to the position ; i. e., crown surface (upslope side of the slab), stauch wall (downslope side), flank surface (lateral side) and bed surface (bottom) (Perla & Martinelli 1976). The neighboring snow or ground of the slab supports the slab from sliding down the slope by tensile, compressive and shear strength of snow and friction between snow and the ground across the boundary. If a snow slab on a slope loses these supports as a result of fracture of the boundaries, a slab avalanche is released.

Fractures of slab boundaries do not necessarily take place simultanelously all over the boundaries. In the case of the ground avalanche which is a full-depth slab avalanche, it is clearly observed that snow fracture along the crown surface takes place primarily, appearing as a large tension crack. Then, deformation of the slab comes about as a result of its glide motion, appearing as surface pleats and undulations ; and finally a ground avalanche is released (Shoda 1967, Narita & Shimizu 1974, 1975, 1976, 1977). The lapse of time required for an avlanache release form the time of appearance of the primary tension crack varies greatly depending upon the condition. Generally, it is from a few hours up to several days for the ground avalanche, but sometimes a tension crack remains at the crown surface until the time of snow melt, even having spread its width but without an avalanche release. (In the case of a superficial slab avalanche, it is released almost the moment that a tension crack appeared.)

The crown surface (wall of the tension crack) shows two kinds of features accoridng to the condition. Generally, a crown surface appears as a clearly cut plane surface perpendicular to the slope, as if it was caused by brittle fracuture of the snow cover. This is a fairly well-known fact. Sometimes, however, the crown surface appears as a rugged and irregular cut end, which shows that microcracks were scattered in snow near the tension crack. It looks as if the snow cover was torn off by ductile fracture. This is a newly

noticed fact which has not been reported. It is reasnoably considered from these observations that tensile fracture of snow across the crown surface of a snow slab on a slope plays a fairly important role in the releasing mechanism of a slab avalanche.

A large number of researches have been conducted on the behavior of snow under tensile stress as follows : Shinojima (1962) made a research on the creep of snow by a tensile experiment with the strain rate of the order of $1.6\times10^{-7}s^{-1}$. Several investigators (Keeler & Weeks 1967, Keeler 1969, Martinelli 1971, Sommerfeld 1971) carried out "spin-tests" of snow actively to measure the tensile strength of snow, but the strain rates of the tests were not made clear. Salm (1971) deduced a failure criterion of snow by tension and compression from a laboratory experiment on strain rates in the range of $\dot{\varepsilon}>1.6\times10^{-3}s^{-1}$. McGabe & Smith (1978), using a testing instrument for the tensile strength of snow, made six experiments in the range of $\dot{\varepsilon}=0.5\sim5.0\times10^{-5}s^{-1}$. However, the strain rates they used were sporadic ones and in a limited range, because they had a practical aim mainly to obtain the tensile strength of snow ; so, the result failed to provide basic information on the mechanism of fracture of snow.

Thus, the author intended to make fundamental researches on the behavior of snow under tensile stress in terms of deformation and fracture in a wide range of strain rates so that he was able to use the result for a sufficient discussion on the releasing mechanism of a slab avalanche. Having initiated an experiment of snow under tensile stress in 1977 (Narita 1980), he continued the experiment totaling 210 in number, under the condition as follows : the temperature and the strain rate, to which snow specimens with a density from 240～470 $kg\cdot m^{-3}$ were subjected, ranged from $-2.5°\sim-18°C$ and $5.5\times10^{-7}\sim2.5\times10^{-3}s^{-1}$, respectively. Besides, in order to validate the fracture condition obtained from the laboratory experiment in which small-sized specimens were used, he conducted a field experiment. Both the experiments were carried out at the Avalanche Observatory, located in Toikanbetsu in northern Hokkaido, of the Institute of Low Temperature Science, Hokkaido University, and in the vicinity of the Observatory.

II. Uniaxial Tensile Experiment : Types of Deformation and Fracture of Snow

II. 1. *Experiment*

i) Snow Specimen

A total of 210 uniaxial tensile experiments of snow were carried out from January-March in 1977, 1979 and 1981, in the cold laboratory of the Avalanche Observatory, Toikanbetsu, using specimens of fine-grained old snow.

A snow specimen was prepared as follows : To begin whith, a snow block uniform in structure (grain size and density), approximately 30 cm×30 cm×60 cm in dimensions, was

sampled from a natural snow cover near the Observatory. The uniformity of snow structure was assured through a visual examination of a snow plate of 1 cm thick by transmitting light through it at the sampling site. The selected snow blocks were stored in the cold room at −10°C to maintain their initial conditions as good as possible, suppressing metamorphosis of snow.

Then, snow specimens were successively taken out from a stored snow block using a cylindrical metal sampler (5 cm in inner diameter and 12.5 cm in length) in parallel to the snow layer, at least after 24 hours of storing but not later than 30 days.

ii) Instrument and Experiment

The instrument used for the tensile experiment of snow, shown schematically in Fig. 1, can provide the crosshead with different constant deformation speeds between 6.8×10^{-8} and 3.1×10^{-4}m・s^{-1}. The ascending speed of the rod was controlled by the decelerator 5 and the reduction gears X and Y, in Fig. 1. For the tensile experiment of snow, 18 different constant speeds were selected, ranging from 6.8×10^{-8} to 3.1×10^{-4}m・s^{-1}, which corresponded to the average strain rates of the specimens approximately from 5.5×10^{-7} to 2.5×10^{-3}s^{-1}. The tensile force was measured by a load cell with a capacity of 2×10^{3}N or 5×10^{2}N, depending

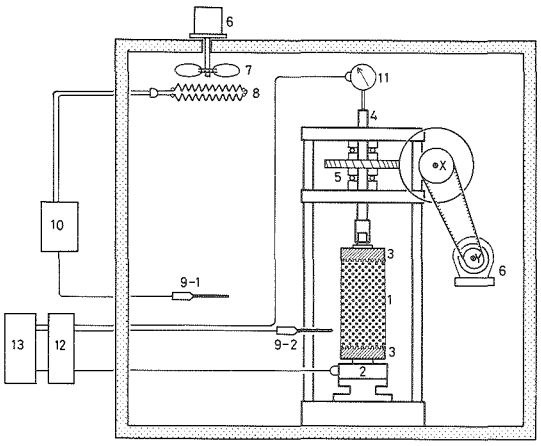

Fig. 1 Schematic diagram of the instrument of tensile experiment of snow.
1 : snow specimen, 2 : load cell, 3 : connector, 4 : ascending rod, 5 : decelerator, 6 : motor, 7 : fan, 8 : electric heater, 9 : thermometer, 10 : thermo-regulator, 11 : dial gauge, 12 : amplifier, 13 : recorder, X & Y : decelerating gears.

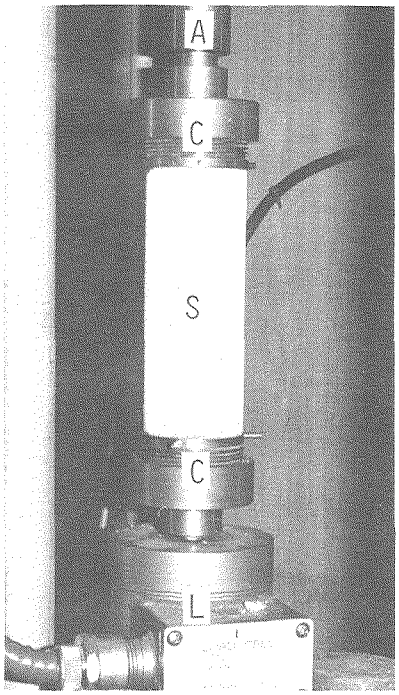

Fig. 2 A snow specimen mounted on the instrument. S : snow specimen, C : connector, A : ascending rod, L : load cell.

upon the snow density. Also, displacement of the crosshead was measured with a dial-gauge to check things such as whether the crosshead was moving properly. The tensile force and displacement of the crosshead were recorded continuously on a trip chart during the experiment.

The instrument was installed in a thermally insulated box, which was placed in the cold laboratory kept at −20°C. Inside of the box was kept at a specific temperature between 0 and −20°C, using an electric heater, a stirring fan and a thermo-regulator. The temperature inside the box was also recorded simultaneously on a trip chart.

A connector was fixed at each end of a snow specimen by the freezing method ; the specimen was then mounted on the apparatus between the load cell and the ascending rod, as shown in Fig. 2. Each connector had a series of concentric circular grooves (1 mm both in width and depth) with the interval of 1 mm on the contact surface with snow for increasing the contact surface area with the snow specimen. When the connectors were fixed, the axis of the specimen had to coincide precisely with those of the rod and the load cell through the connectors. For that purpose, the specimen and the top and the bottom connector were placed, before they were fixed, horizontally on a guide rail with a straight V-shaped groove in the order : the top connector, the specimen, the bottom connector ; then, they were brought to contact with each other by sliding the connectors along the groove. At this stage, if the temperature of the connectors was about +0.5°C, it melted both the cut ends of the snow specimen by a thickness of 1~1.5 mm and no more. Allowing the specimen to stand as it was for a while, the connectors were each tightly fixed on each cut end of the specimen maintaining a common axis with the specimen by the freezing of the meltwater which had filled up the circular grooves of the connectors. The meltwater did not penetrate into the body of the specimen. This procedure was conducted in the cold laboratory kept at −10°C.

Temperatures at which the experiment was conducted were −2.5°, −6°, −10° and −18° C. So, a series of tests was carried out check the thermal equilibrium of a snow specimen, which was initially kept at −10°C, with the air and instrument, which were different in temperature from the initial temperature of the specimen. As a result, it was confirmed that the specimen attained a thermal equlibrium in shorter than 50 minutes, even in case of a largest temperature difference amounting to 8°C. Therefore, a tensile experiment was started one hour, at least, after the specimen was mounted on the apparatus in the box at a specified temperature.

II. 2. *Tensile Deformation and Local Strain of Snow*

Although snow with an apparently uniform structure was subjected to a uniaxial tensile experiment at the constant speed of the crosshead, it was not obvious whether or not uniform strain took place all over the specimen and whether or not values of displacement and speed of the crosshead enabled the calculation of the real strain and strain rate of snow, respectively. To make them obvious observations were made, in some detail, of the real

deformation of snow in the local domain of the specimen by the following experiment.

In advance of the experiment the specimen was graduated exery 1 cm on the lateral side parallel to the axis by stenciling the lines with colcothar powder, as shown in Fig. 3. During the experiment, deformation of the graduations was intermittently photographed and measured. Then the local strain of the specimen was calculated taking exery other graduations as the boundaries of a local domain. The local strain was calculated by comparing the original distance between every other graduations as the intial length with the transformed distance at every measurement as the final length. The result is given in Fig. 4.

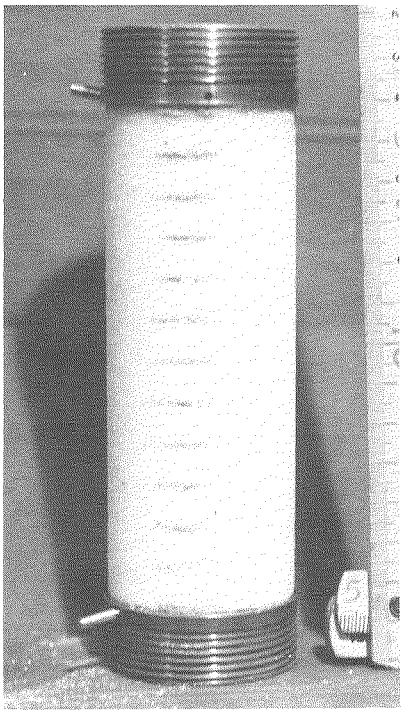

Fig. 3 Graduated snow specimen. (1 cm graduation)

As seen clearly in the diagrams, the local strain which took place was not uniform all over the specimen ; moreover, a dispersion in local strain increased as the deformation of the specimen progressed (Fig. 4 (a)). If the specimen was slowly extended, the dispersion of the local strain was considerably small even in case of large strain (Fig. 4 (b)). In Fig. 5, the standard deviation of the local strain was plotted against the apparent strain of the whole body of the specimen in the crosshead $\bar{\varepsilon}$. This result shows clearly the tendency of the local strain described above, though the data obtained for a small strain rate are not sufficient to warrant a conclusion.

Thus, the local domain of a snow specimen behaves unsystematically even under uniaxial tensile stress, which is caused possibly by uniformless distributions of mechanical property and invisible nucleus of fracture in snow texture, as shown by observations of thin sections. Moreover, nobody can estimate the real local strain from a displacement in the crosshead of the specimen, i. e., the deformation of the whole body of the specimen.

Here, when characterizing the experimental condition, the author defined the strain of a specimen, $\bar{\varepsilon}$, by the apparent strain of the specimen in the crosshead ; so, in this paper the strain of a specimen does not necessarily coincide with the real local strain.

II. 3. *Types of Deformation and Fracture of Snow under Tensile Stress*

At the beginning, snow of the density ρ was subjected, at -10°C, to the strain rate $\dot{\bar{\varepsilon}}$ in a uniaxial tensile experiments, ρ and $\dot{\bar{\varepsilon}}$ ranging from 290～310 kg・m^{-3} and 5.5×10^{-7}～2.5×10^{-3}s^{-1}, respectively. The experiment led to the classification of four general types con-

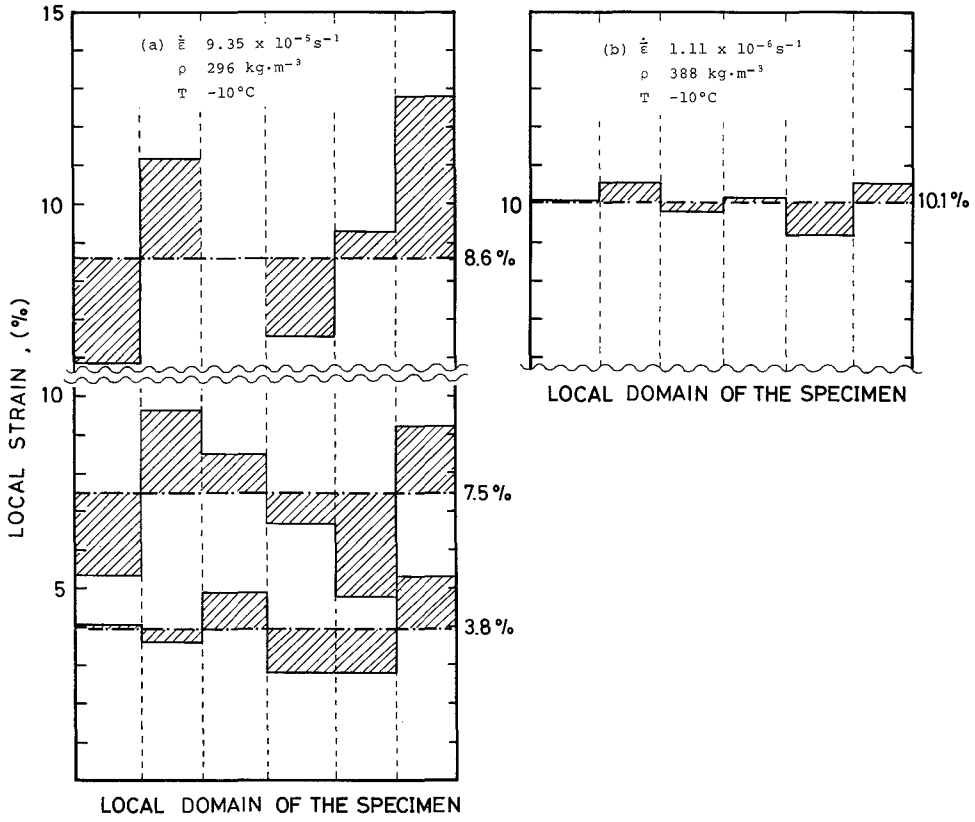

Fig. 4 Distribution of the local strain of snow under uniaxial tensile stress. Chain line indicates the strain of the specimen in the crosshead $\bar{\varepsilon}$.

cerning deformation and fracture of snow, i. e., types a, b, c and d, depending upon the strain rate $\dot{\bar{\varepsilon}}$, as shown in Fig. 6. The followings give the description and definition of each type :

i) Type a : When a snow specimen was extended at a strain rate in the range of $2.4\times10^{-4}<\dot{\bar{\varepsilon}}<2.5\times10^{-3}s^{-1}$, the resisting force of snow to extension increased linearly with an increase in strain, until the specimen suddenly broke up at a strain of 0.15~0.30%, the largest being 0.8%, as shown in Fig. 7. The cut end of the fracture was sharp and perpendicular to the direction of tension, but observations of thin sections showed no noticeable change in structure of snow, as compared with the initial state. Although the deformation of snow up to the time of fracture looked to be "elastic" by an apparent linear relation between resisting force and strain, it was actually a "visco-elastic" deformation, and the fracture was "brittle fracture". This type of deformation/fracture of snow was classified as "type a" in this paper (Figs. 6 and 7).

Strength of snow R in the case of "type a" was defined by the largest resisting

force to extension by which the snow specimen was broken up.

ii) Type b : When a snow specimen was extended at a strain rate of $7.0\times10^{-5}<\dot{\bar{\varepsilon}}<2.4\times10^{-4}s^{-1}$, it was not broken up in the linear visco-elestic region OC, and behaved viscously in the region beyound point C sustaining a fairly constant resisting force to extension, as shown in the diagram of Fig. 8. At point K, the resisting force began to decrease obviously, leading to fracture at F. Characteristic appearances of this type of deformation/fracture were the formation of "microcracks" in the specimen and the feature of fracture. On the way of the viscous deformation CK, microcracks appeared perpendicularly to the direciton of

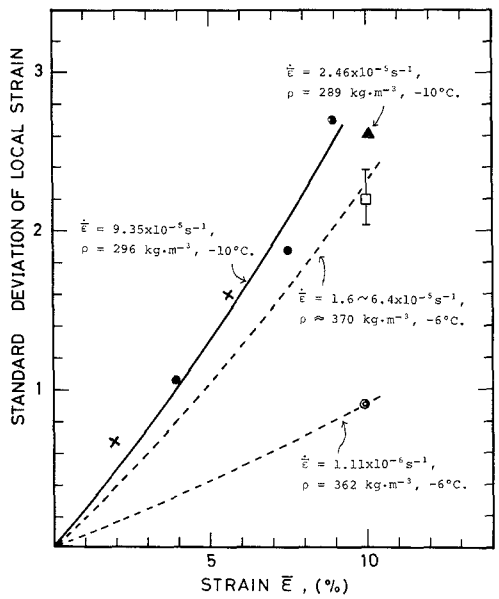

Fig. 5 Standard deviation of the local strain of snow under uniaxial tensile stress.

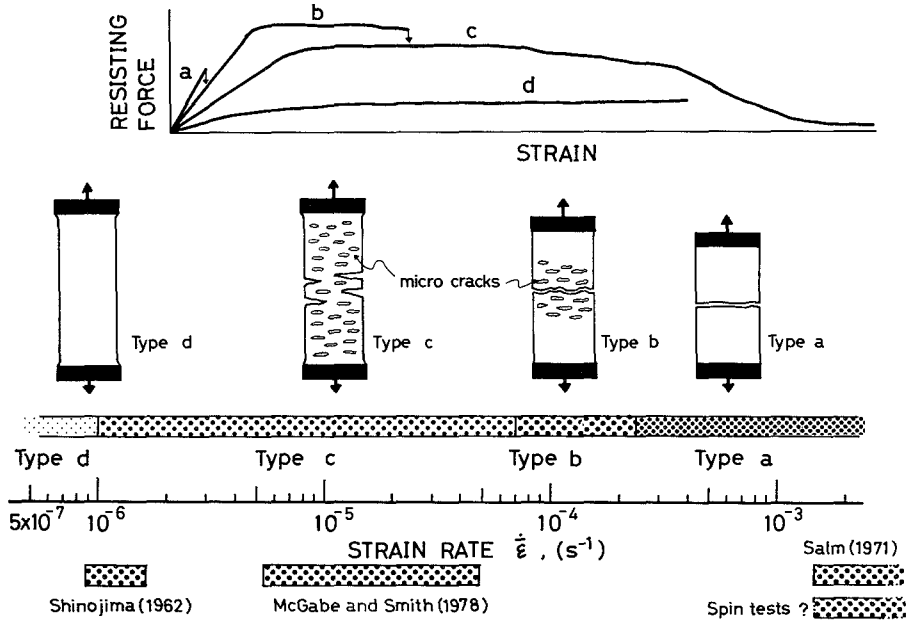

Fig. 6 Four types of deformation and fracture of snow under uniaxial tensile stress.

tension in a limited zone near the central part of the specimen. When the deformation came close to K, an indication of fracture appeared in the area of microcracks, as seen in photograph (2) of Fig. 8. The indication of fracture grew to a distinct crack and stretched the width fairly quickly as the deformation increased, and finally attained to the fracture of the specimen. Compared with that of the brittle fracture of type a the cut end of the fracture showed a rather rugged surface. As this fracture was very similar to a specific type of fracture in metallurgy, this was called "ductile fracture" in this paper. This type of deformation/fracture of

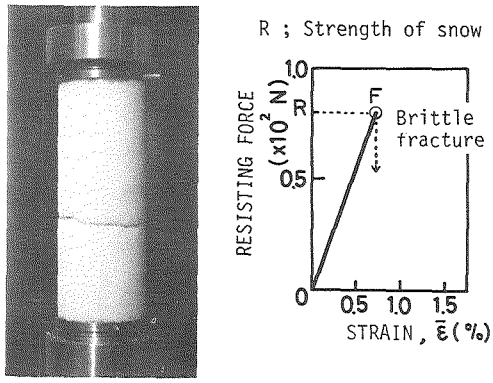

Fig. 7 Deformation/fracture of snow, type a.
($\dot{\bar{\varepsilon}}=8.33\times10^{-4}s^{-1}$, $\rho=370$ kg·m^{-3}, T$=-10$°C)

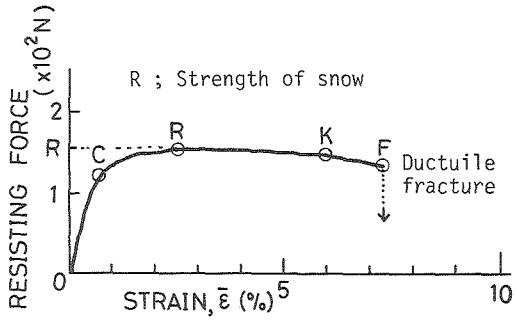

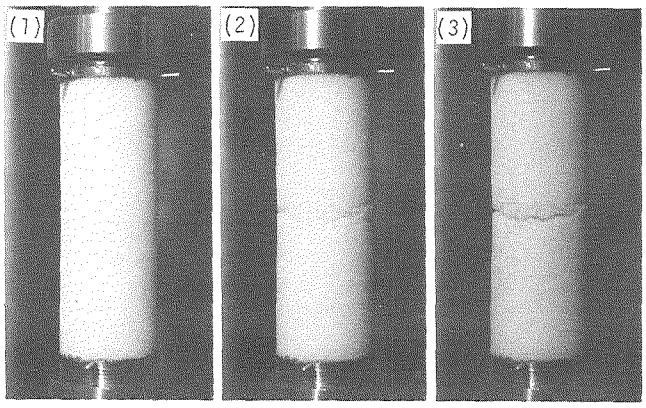

Fig. 8 Deformation/fracture of snow, type b.
($\dot{\bar{\varepsilon}}=9.15\times10^{-5}s^{-1}$, $\rho=298$ kg·m^{-3}, T$=-10$°C)

snow was classified as "type b".

Strength of snow R in the case of type b was defined by the maximum resisting force of snow to extension which appeared in the viscous region CK.

iii) Type c : When a snow specimen was extended at a strain rate of $1.0\times10^{-6}<\dot{\bar{\varepsilon}}<7.0\times10^{-5}s^{-1}$, it behaved also viscously like type b in the region beyond C. But it was never torn off even by a large strain of $\bar{\varepsilon}=23.3\%$, while a remarkable failure appeared on the specimen near the end of the experiment, as shown in the photographs of Fig. 9. The resisting force of snow to extension began to decrease very slowly on the way to K, obviously at K, and very remarkably at G, in the diagram of Fig. 9. The most characteristic appearances of this typje of deformation/failure process was the formation of microcracks in the specimen and the feature of failure. On the way of the viscous deformation CG, microcracks appeared perpendicularly to the direction of extension all over the specimen. They increased their number and size as the extension proceeded. In the region beyond G, an indication of fracture appeared at several places in the specimen, and they grew to large cracks connecting several microcracks with each other. However, the specimen was never torn off even by a large strain of

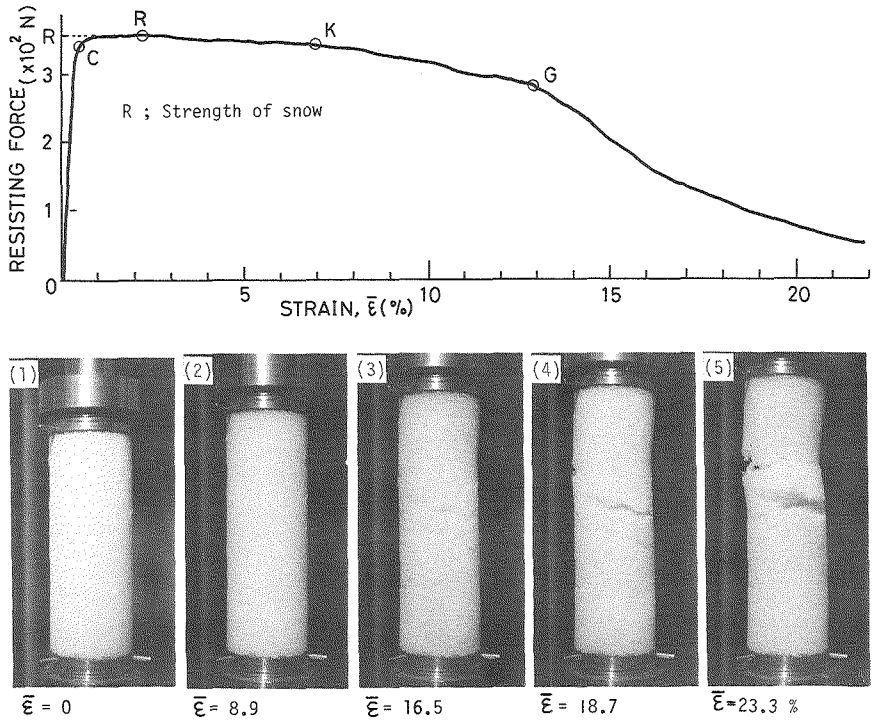

Fig. 9 Deformation/fracture of snow, type c.
($\dot{\bar{\varepsilon}}=2.96\times10^{-5}s^{-1}$, $\rho=455$ kg · m^{-3}, $T=-10°C$)

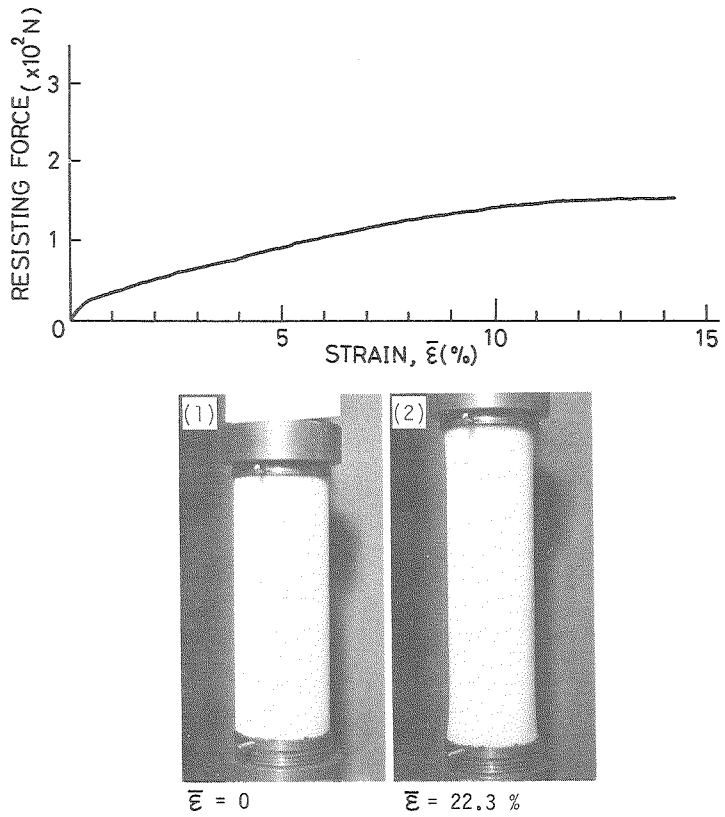

Fig. 10 Deformation of snow, type d.
($\dot{\bar{\varepsilon}}$=9.54 x $10^{-7}s^{-1}$, ρ=337 kg・m^{-3}, T=−10℃)

23.3%, as shown in the photographs of Fig. 9. It took 2.2 hours from the start of this experiment to attain to the strain of $\bar{\varepsilon}$=23.3%, i. e., from the photographs (1) to (5) of Fig. 9. Continuing this experiment further, the specimen would also be torn off by ductile fracture. This type of deformation/failure of snow was classifed as "Type c".

Strength of snow R in the case of type c was defined by the maximum resisting force of snow to extension which appeared in the region beyond C.

iv) Type d : When a snow specimen was extended at a strain rate of $5.5\times10^{-7}<\dot{\bar{\varepsilon}}<1.0\times10^{-6}s^{-1}$, it behaved as a viscous substance, increasing the length and decreasing the diameter uniformly with neither fracture nor microcracks as the extension proceeded, even by a large strain of $\bar{\varepsilon}$=22.3%, as shown in the photographs of Fig. 10. The resisting force of the snow to extension increased very gradually as the strain $\bar{\varepsilon}$ increased, as shown in the diagram of Fig. 10. This type of deformation was classified as "type d". The deformation of snow of type d is "creep" as far as no failure appears,

at least up to $\bar{\varepsilon}=22.3\%$ in this experiment.

II. 4. *Density Dependency of the Behavior of Snow under Tensile Stress*

The first series of tensile experiments of snow was carried out under conditions of the constant snow density (290～310 kg · m^{-3}) and the constant temperature (−10°C), in the range of 5.5×10^{-7}～$2.5\times10^{-3}s^{-1}$ in strain rate, to obtain the general view of the behavior of snow under tensile stress. To investigate the density dependency of the behavior of snow under tensile stress, the second series of tensile experiments of snow was carried out. In this series, the density of snow was ranged from 245～466 kg · m^{-3}, while the temperature was keept at −10°C. The strain rate covered the range from 5.5×10^{-7}～$2.2\times10^{-3}s^{-1}$. The strength of snow was measured by the definition described in II. 3. The results were plotted in the diagram of strain rate $\dot{\bar{\varepsilon}}$ versus strength of snow R together with the type of deformation/fracture of snow, as shown in Fig. 11. As seen on the diagram, the strength of snow increased fairly rapidly with a decrease in strain rate in the region of brittle fracture (type a), while it decreased rather gradually in the regions of ductile deformation/fracture

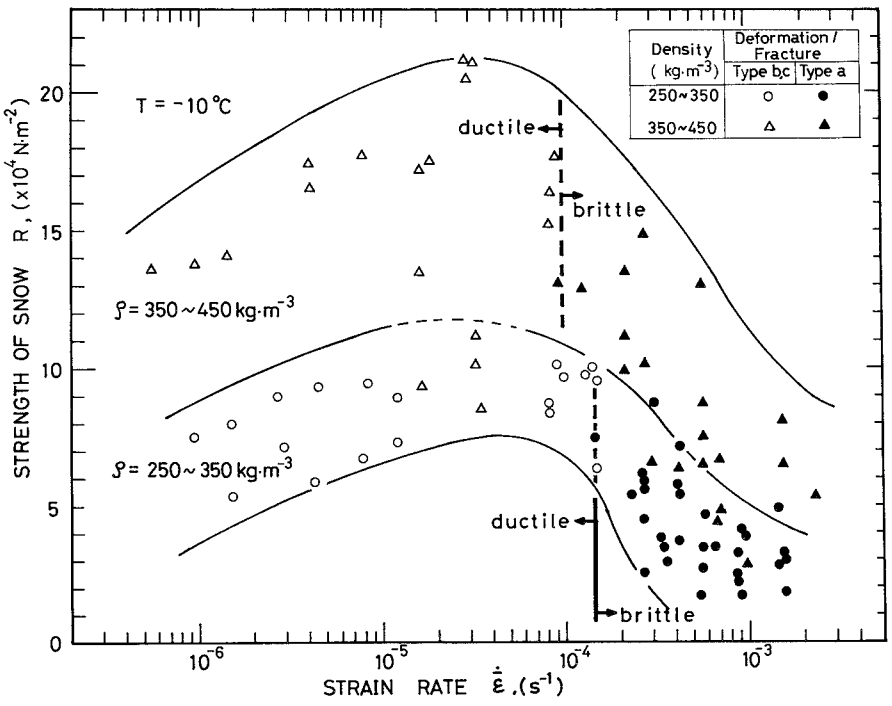

Fig. 11 Density dependency of tensile strength of drifted snow, and transition from brittle fracture to ductile fracture.

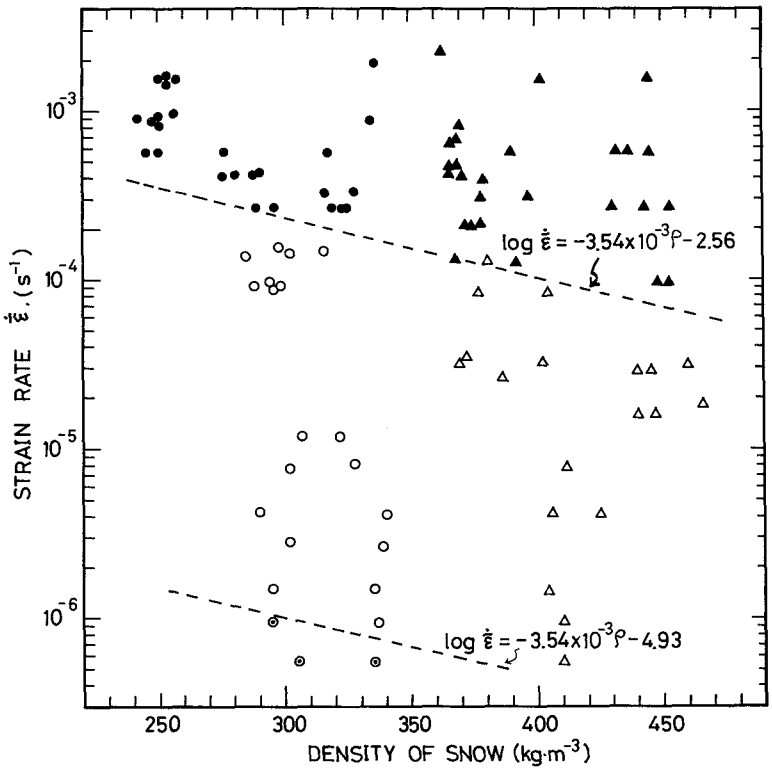

Fig. 12 Density dependency of behavior of drifted snow under tensile stress. (The same symbols as in Fig. 11 are used.)

(types b and c).

Regarding the effect of the snow density on the strength of snow, one can see a general tendency that the strength of snow increases with increasing snow density. However, the density dependency is rather broad. It is considered that the strength of snow does depend not only on its density, but also on its structure, i. e., diameter, length, orientation and number of ice bonds connecting the snow grains with each other ; the strength of snow vaires considerably with the structure even for specimens of the same density. The structure is likely to have a predominant effect on the strength of snow rather than the density itself. However, the author took the density as one of the parameters of the strength of snow for the first approach to investigate the snow strength, as we do not have any other appropriate ways to describe the snow structure precisely at the present time. This fact must have brought about such a rather broad dependency of the strength of snow on the density.

Plotting the experimental results on a $\rho - \dot{\bar{\varepsilon}}$ diagram, the types of deformation/fracture of snow were clearly specified by the range of strain rates, as shown in Fig. 12. Namely,

brittle fracture (type a) took place at strain rates above $2.3\times10^{-4}s^{-1}$ at the denisty of 300 kg · m^{-3}, and the boundary for the strain rate of transition from type a to type b descended with an increase in density. Accordingly, the brittle fracture condition is,

$$log\ \dot{\varepsilon} > -3.54\times10^{-3}\cdot\rho - 2.56, \tag{1}$$

Where $\dot{\varepsilon}$ is the strain rate (s^{-1}) and ρ is the snow density (kg · m^{-3}). Equation (1) suggests that brittleness of snow increases with an increase in snow density or strain rate.

Ductile behavior (types b and c) appeared in the range from about $1\times10^{-6}s^{-1}$ to 2.3×10^{-4} s^{-1} at the density of 300 kg · m^{-3}. The number of data of type d obtained were three in the experiments of this series, and the boundary between types d and c was given by the condition under which type d took place, as the following equation :

$$log\ \dot{\varepsilon} < -3.54\times10^{-3}\cdot\rho - 4.93. \tag{2}$$

Equation (2) suggests that plasticity of snow increases with a decrease in snow density or strain rate.

II. 5. *Temperature Dependency of the Behavior of Snow under Tensile Stress*

Another tensile experiment of snow was made to look into the temperature dependency

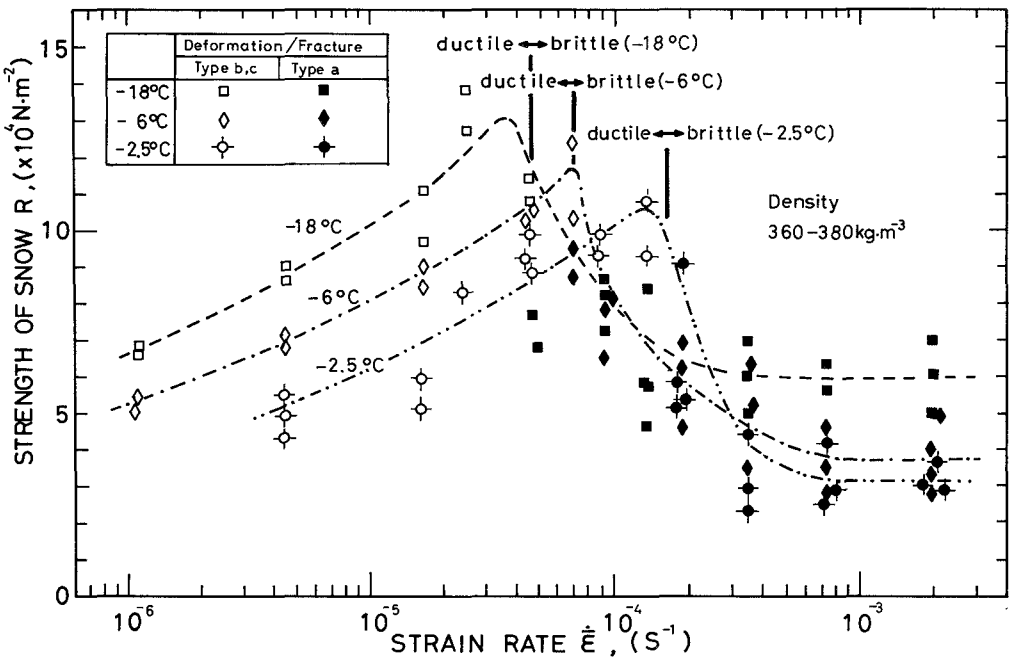

Fig. 13 Temperature dependency of tensile strength of calmly deposited snow, and transition from brittle fracture to ductile fracture.

of the behavior of snow under tensile stress, with the density of snow ranging from 360~380 kg · m^{-3}, the temperatures at −2.5°, −6° and −18°C, and the strain rates covering the range form $1.1\times10^{-6}\sim2.2\times10^{-3}s^{-1}$. The strength of snow was also measured. The relation between the strain rate and the strength of snow is shown in Fig. 13. The temperature dependency of the strength of snow under tenisle stress appeared very clearly in contrast with the density dependency. The strength of snow sustained a remarkably constant value in the higher region of brittle fracture (type a) and rapidly increased in the lower region, as the strain rate decreased. In the transitional region from brittle fracture to ductile deformation/fracture, the strength of snow attained to the maximum value ; then it decreased rather gradually with a decrease in strain rate in the ductile behavior region. Besides, the position of the maximum strength of snow shifted toward to lower strain rate, whereas the value of it increased with lowering temperature.

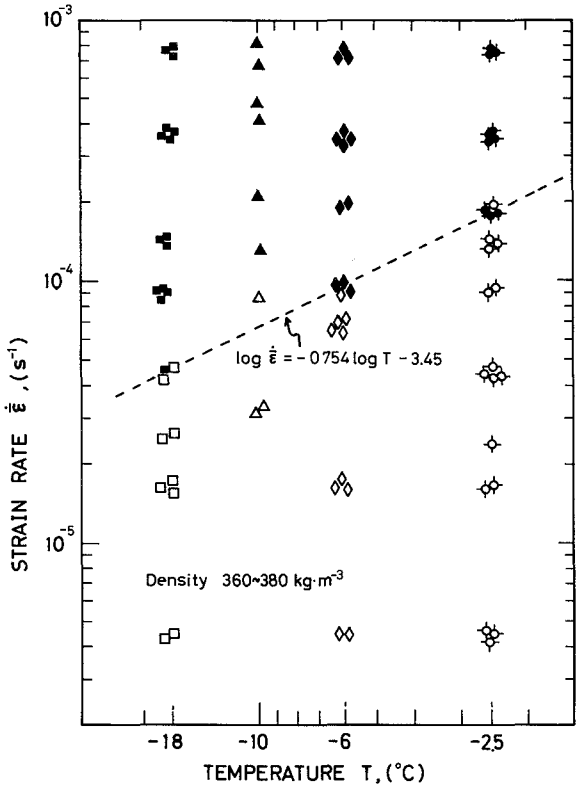

Fig. 14 Temperature dependency of behavior of calmly deposited snow under tensile stress. (The same symbols as in Fig. 13 are used.)

A comparison of the $\dot{\bar{\varepsilon}}-R$ curves given in Figs. 11 and 13 shows some different general shapes from each other, though they should accord exactly with each other if the conditions of the specimen and experiment coincided. The reason of such a disaccordance in the $\dot{\bar{\varepsilon}}-R$ curves was considered to originate from a structural difference in snow specimens. As for snow used in the experiments, it was drifted snow for the former series and calmly deposited snow for the latter series. Observations of thin sections of these two kinds of snow showed some structural difference between them ; namely, the grain size of the drifted snow was somewhat finer than that of the calmly deposited snow on the average, if they had about the same density. As mentioned in the previous section, the strength of snow varies fairly widely with the structure, even in case of the same density. Therefore, it is considered that such a systematic sampling of snow for the experiments, i. e., drifted snow for the experiments for density dependency and calmly deposited snow for those for temperature depen-

dency, resulted in such a disaccordance in the general shapes of the $\dot{\bar{\varepsilon}}-R$ curves between these two series. Further experiments are necessary to clarify this disaccordance.

Plots of experimental results of this series on the diagram of temperature versus strain rate ($T-\dot{\bar{\varepsilon}}$ diagram), show a fairly clear boundary between the brittle fracture and ductile fracture of snow, as shown in Fig. 14. Accordingly, the brittle fracture condition is,

$$\log \dot{\bar{\varepsilon}} > -0.754 \log T - 3.45, \tag{3}$$

where $\dot{\bar{\varepsilon}}$ is the strain rate (s^{-1}) and T is the temperature (°C). Equation (3) suggests that brittleness of snow increases with lowering temperature and increasing strain rate.

III. Formation of Microcracks in Snow under Tensile Stress

III. 1. *Field Observation of Microcracks appearing in a Snow Cover on a Slope*

Field observations were made of microcracks appearing in a snow cover on a slope near tension cracks. Two types of snow fracture making a tension crack were found, as briefly described previously, i. e., "brittle fracture type" and "ductile fracture type".

Figure 15 shows a tension crack of the brittle fracture type. The cut end of the fracture is fairly straight and smooth, being perpendicular to the slope. No noticeable change was in structure of snow in the region near the crack, compared with that of ordinary snow away from the crack, even by observations of thin sections. This type of the cut end keeps its clear-cut shape for a fairly long time, even after the widening of the crack width.

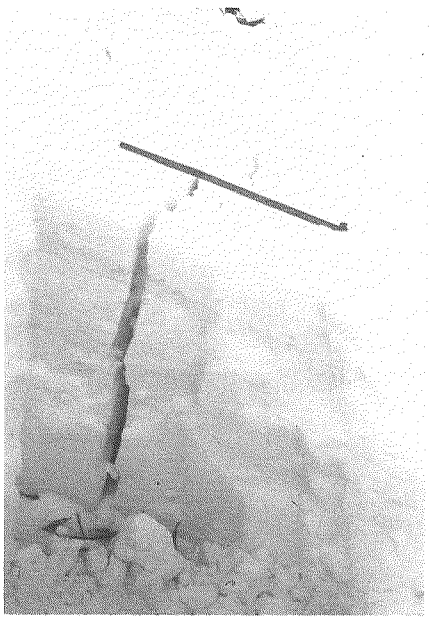

Fig. 15 Tension crack of the brittle fracture type.

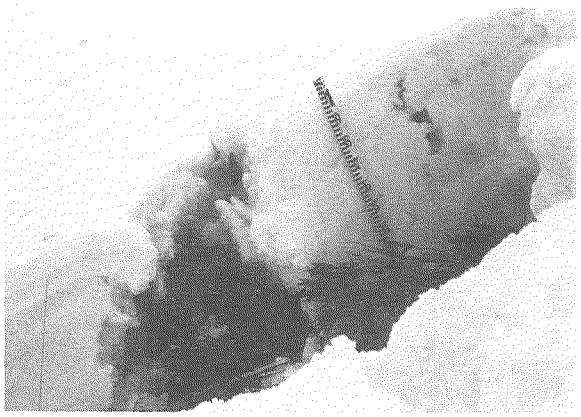

Fig. 16 Tension crack of the ductile fracture type.

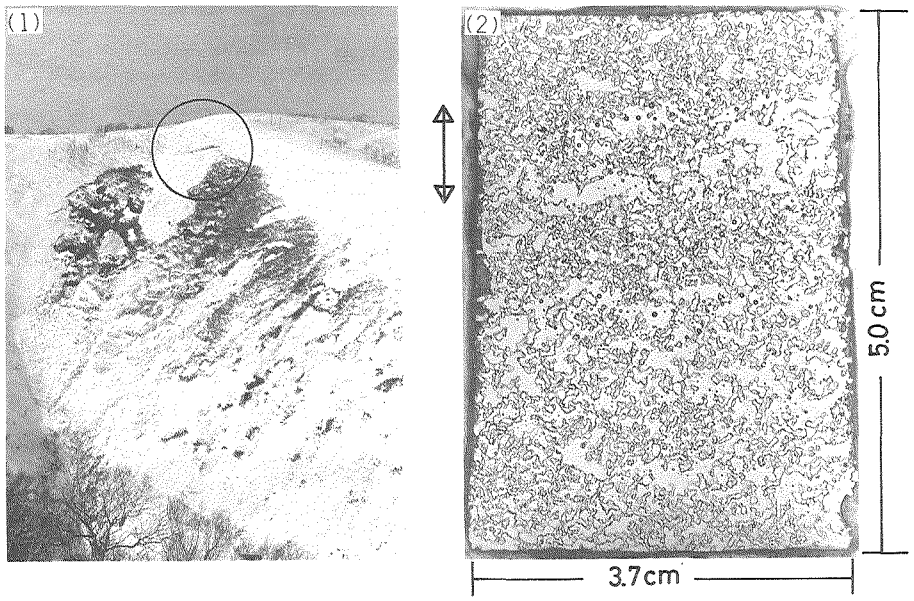

Fig. 17 Microcracks which appeared in a natural snow cover on a slope.
(1) Location of the tension crack (at the center of the circle). (2) Thin section of snow sampled at 30 cm upslope of the tension crack. Thin section was prepared in parallel to a snow layer. (Arrow mark indicates the direction of the maximum slope.)

Figure 16 shows a tension crack of the ductile fracture type. The cut end of the fracture is rugged and irregular, and small cavities of several centimeters in diameter were observed scattering in snow near the crack.

A snow block was sampled from a position about 30 cm upslope side of a tension crack (ductile fracture type), which appeared in the circle on photograph (1) of Fig. 17, and thin sections of the snow were observed. A thin section of the snow was prepared in parallel to the snow layer. As seen clearly in photograph (2) of Fig. 17, microcracks of the order of millimeters in width and millimeters~centimeters in length had appeared on the thin section of the snow roughly perpendicularly to the direction of the maximum slope line. Such a structure in snow is very characteristic and hardly observed in the ordinary snow cover.

A fairly large number of such observations were made ; and it was presumed that these microcracks and small cavities in snow near some tension cracks should have been created when the snow cover was going to be broken up under tensile stress.

III. 2. *Observation on Microcrack Growth in Snow in the Laboratory*

As described briefly in the previous Chapter, microcracks appeared in snow when it was subjected to a tensile deformation of type b or c, i. e., extension at a strain rate of the order

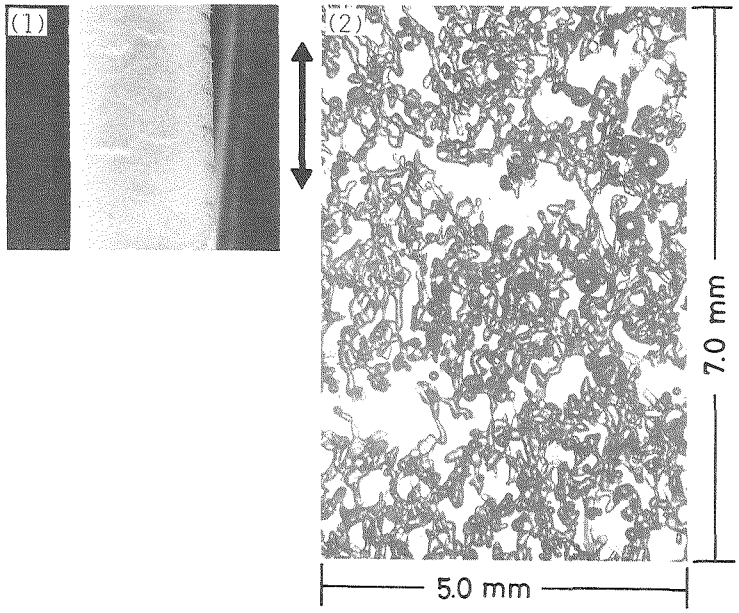

Fig. 18 Microcracks which appeared in a snow specimen after a tensile experiment (deformation type c).
(1) Observation by transmitting light. (2) Thin section of the specimen (Arrow mark indicates the direction of tension).

of $10^{-7}<\dot{\bar{\varepsilon}}<10^{-4}s^{-1}$. Figure 18 gives an example of the microcracks which appeared in a snow specimen subjected to tensile deformation of type c in the laboratory. Positions of the microcracks are approximately perpendicular to the direction of tension, and their shapes are similar and their dimensions are of the same order as those observed in the natural snow cover.

Through these observations on the microcracks, it was considered that the microcracks found in a natural snow cover in the vicinity of tension cracks (ductile fracture type) and that those observed in the snow specimen used for the tensile experiment at the strain rate of the order of $10^{-7}<\dot{\bar{\varepsilon}}<10^{-4}s^{-1}$ were formed by the same mechanism.

III. 3. *Growth Condition of Microcracks in Snow under Tensile Stress*

To investigate the growth condition of microcracks in snow in more detail, the following experiments were conducted :

i) Effect of strain rate : A tensile experiment of snow was carried out using specimens of a constant density, practically ranging from 410～440 kg・m^{-3}, at the constant temperature of −10°C and three different strain rates : $\dot{\bar{\varepsilon}}=9.5\times10^{-7}$; 7.7×10^{-6} ; $4.1\times10^{-5}s^{-1}$. When the strain of the specimen attained to a constant value of $\bar{\varepsilon}\fallingdotseq13\%$, it

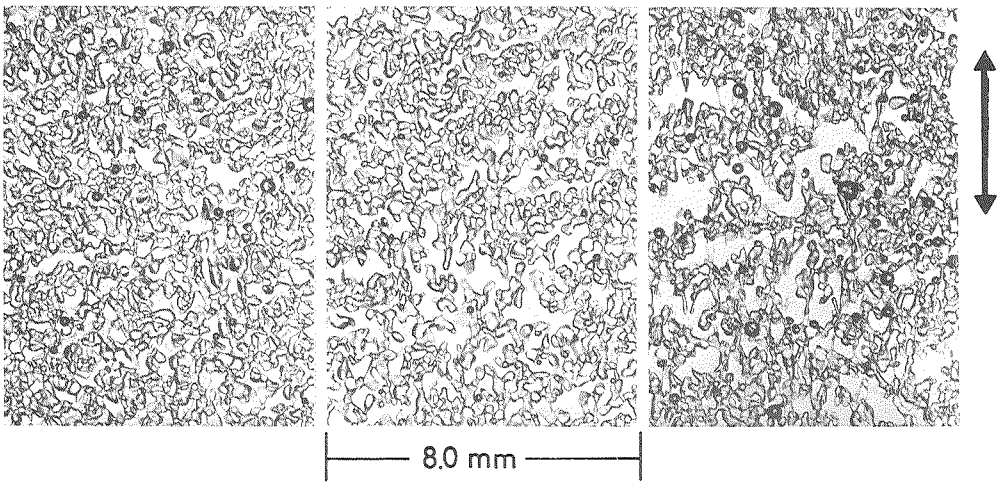

(1) Strain rate $9.5\times10^{-7}s^{-1}$, strain 13.6%, density 440 kg·m^{-3}, temperature -10°C.

(2) Strain rate $7.7\times10^{-6}s^{-1}$, strain 13.3%, density 410 kg·m^{-3}, temperature -10°C.

(3) Strain rate $4.1\times10^{-5}s^{-1}$, strain 12.7%, density 425 kg·m^{-3}, temperature -10°C.

Fig. 19 Effect of strain rate on the microcrack growth in snow under tensile stress, in the laboratory. (Arrow mark indicates the direction of tension.)

stopped extending ; then its thin sections were observed concerning the growth of microcracks. Figure 19 shows the result. As seen on the photographs, the growth of microcracks was fairly evident at a high strain rate ($\dot{\bar{\varepsilon}}=4.1\times10^{-5}s^{-1}$); less evident at a medium strain rate ($\dot{\bar{\varepsilon}}=7.7\times10^{-6}s^{-1}$); and rather obscure at a low strain rate ($\dot{\bar{\varepsilon}}=9.5\times10^{-7}s^{-1}$). The highest strain rate ($\dot{\bar{\varepsilon}}=4.1\times10^{-5}s^{-1}$) of this experiment is close to the upper limit of the type b range in the first series of the previous Chapter, whereas the lowest one ($\dot{\bar{\varepsilon}}=9.5\times10^{-7}s^{-1}$) is close to the lower limit of the type c range in the same series. So, this experiment covered roughly the range of microcrack growth in snow under tensile stress.

This result shows a clear tendency of an increase in growth of microcracks with an increase in strain rate, as far as the strain rate is in the range of ductile behavior of snow.

ii) Effect of temperature : Another tensile experiment of snow was conducted in a similar way to the first one except the strain rate which was kept constant at $\dot{\bar{\varepsilon}}=4.4\times10^{-5}s^{-1}$, and the different temperatures : $T=-2.5°$, $-6°$, -18°C. Density of a snow specimen was $\rho=360\sim370$ kg · m^3, and the experiment was stopped at a constant strain of $\bar{\varepsilon}=10\%$. The resultant photographs of thin sections are given in Fig. 20. From them we can see a weak but certain tendency of an increase in growth of microcracks with lowering temperature, though not so clearly defined as those in the first experiment.

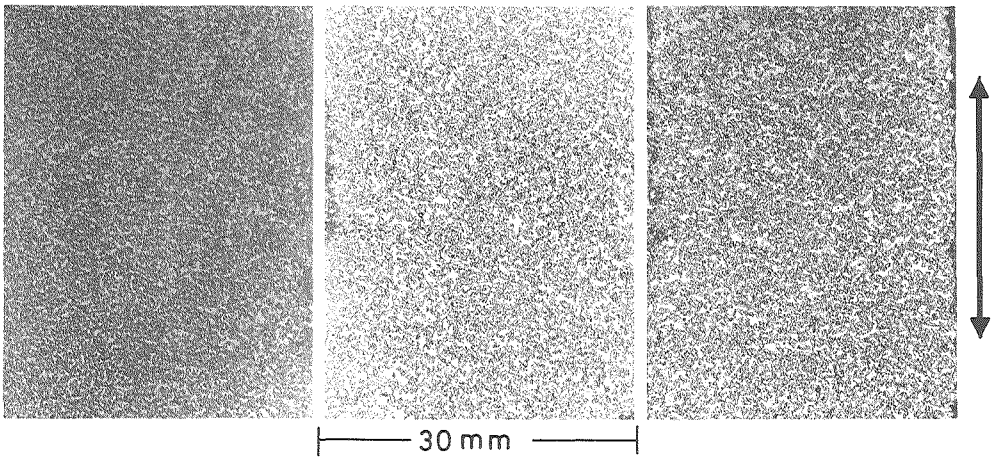

(1) Temperature −2.5°C, strain 9.8%, strain rate $4.40\times10^{-6}s^{-1}$, density 379 $kg\cdot m^{-3}$.

(2) Temperature −6°C, strain 9.9%, strain rate $4.44\times10^{-6}s^{-1}$, density 378 $kg\cdot m^{-3}$.

(3) Temperature −18°C, strain 10.2%, strain rate 4.40×10^{-6} s^{-1}, density 370 $kg\cdot m^{-3}$.

Fig. 20 Effect of temperature on the microcrack growth in snow under tensile stress, in the laboratory. (Arrow mark indicates the direction of tension.)

On the whole, it is concluded that the microcracks grow in snow under tensile stress at a strain rate in the range of the order of $10^{-7}<\dot{\bar{\varepsilon}}<10^{-4}s^{-1}$ and that the growth is more active with increasing strain rate and lowering temperature.

IV. Fracture Condition of Snow

IV. 1. *Critical Strain and Fracture Condition of Snow*

In the tensile experiments of ductile deformation of snow (types b and c), the maximum resisting force of snow to extension appeared at a strain beyond the yield point. The resisting force decreased very gradually beyond the maximum point immediately or after sustaining the maximum value for a while.

It was considered that the nucleation and growth of the microcracks in snow resulted in this gradual decrease in resisting force. In this connection, the author defined the nucleation of microcracks as the beginning of fracture of snow, and the ultimate tensile strain without microcracks as the critical strain $\bar{\varepsilon}_c$, which coincides with the strain at the instant of the beginning of a decrease in resisting force from the maximum value. In other words, fracture of snow under tensile stress begins at the critical strain $\bar{\varepsilon}_c$ by nucleation of microcracks.

From this standpoint, the critical strain of snow was plotted against strain rate as shown

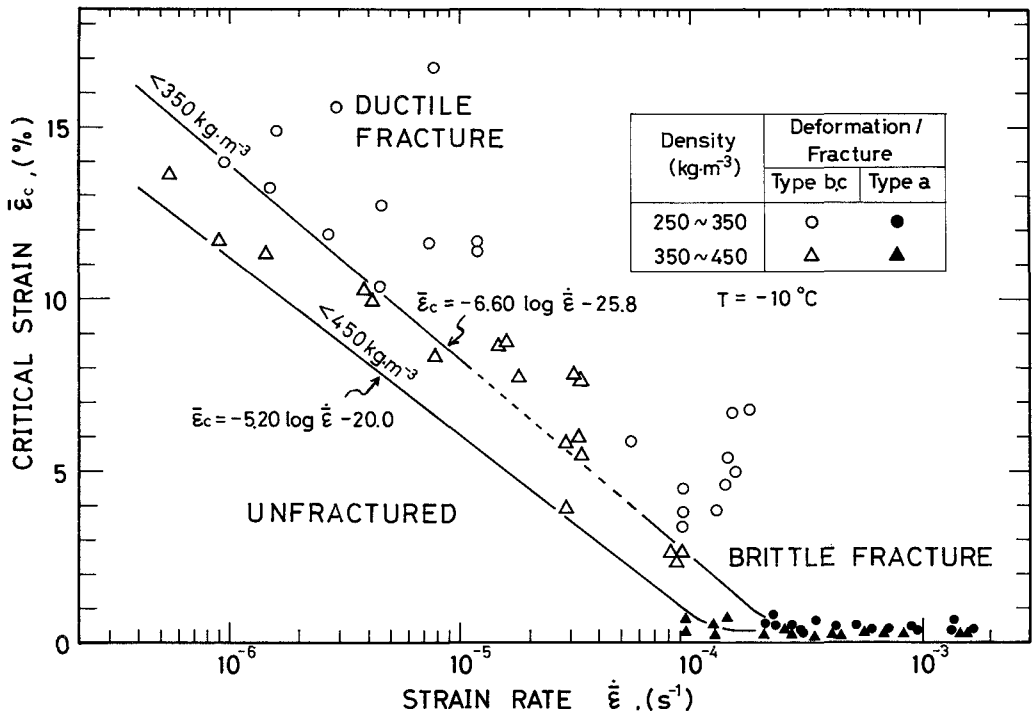

Fig. 21 Density dependency of critical strain $\bar{\varepsilon}_c$ of drifted snow. (The fracture condition of snow I)

in Fig. 21. Brittle fracture took place at the critical strain, less than 0.5 %, regardless of the strain rate down to approximately $1\times10^{-4}s^{-1}$. Then the critical strain increased with a decrease in strain rate at least down to $5\times10^{-7}s^{-1}$. As for the broad density dependency of the critical strain of snow it can be observed that the critical strain increases with a decrease in density of snow.

Two solid lines in Fig. 21 give the lower limits of nucleation of microcracks in snow, one for 450~350 kg · m^{-3} and the other for 350~250 kg · m^{-3} in density range. This means that the microcracks can be nucleated in snow in the region above the corresponding solid line. Accordingly, the fracture condition of snow, defined by nucleation of microcracks, can be given for drifted snow at −10°C as follows: Namely, fracture of snow starts in the region of,

$$\bar{\varepsilon} > -5.20 \log \dot{\bar{\varepsilon}} - 20.0,$$
$$(\text{for } \rho < 450 \text{ kg} \cdot \text{m}^{-3};\ 5.5\times10^{-7} < \dot{\bar{\varepsilon}} < 9.5\times10^{-5}s^{-1}), \quad (4)$$
$$\bar{\varepsilon} > -6.60 \log \dot{\bar{\varepsilon}} - 25.8,$$
$$(\text{for } \rho < 350 \text{ kg} \cdot \text{m}^{-3};\ 5.5\times10^{-7} < \dot{\bar{\varepsilon}} < 2\times10^{-4}s^{-1}), \quad (5)$$

where $\bar{\varepsilon}$ is the tensile strain (%), $\dot{\bar{\varepsilon}}$ the strain rate (s^{-1}) and ρ the snow density. The density of 450 kg · m^{-3} is a considerably high value for natural seasonal snow. And as the critical

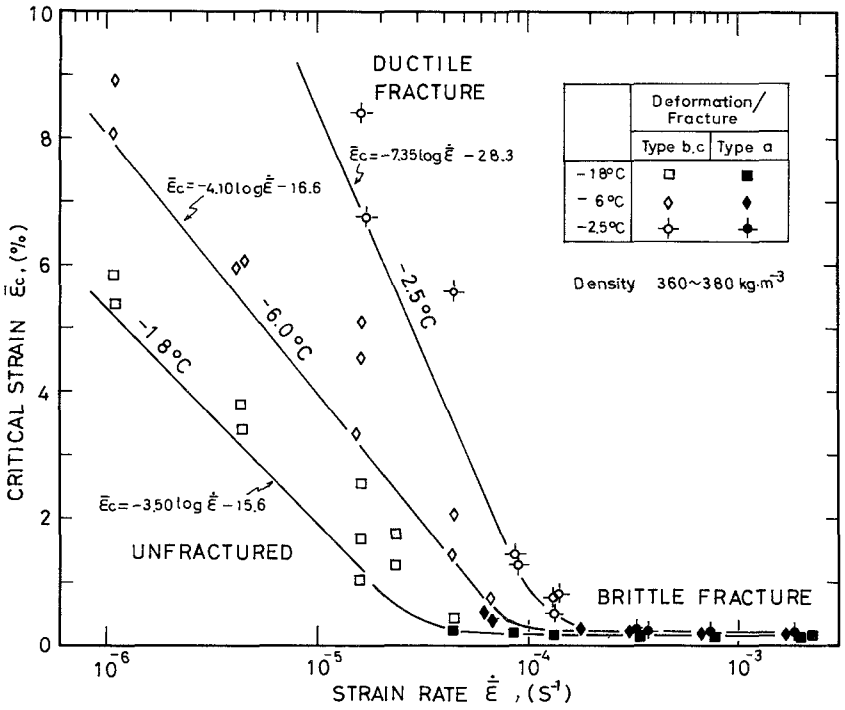

Fig. 22 Temperature dependency of critical strain $\bar{\varepsilon}_c$ of calmly deposited snow. (The fracture condition of snow II)

strain of snow with smaller density appears larger, it is considered that eq. (4) is valid for the most of drifted snow.

The temperature dependency of the critical strain of calmly deposited snow appeared fairly clear as shown in Fig. 22. Namely, the critical strain increase with rising temperature. Accordingly, the fracture condition of calmly deposited snow of 360~380 kg · m^{-3} in density is given as follows : Namely, fracture of snow starts in the region of,

$$\bar{\varepsilon} > -7.35 \log \dot{\bar{\varepsilon}} - 28.3,$$
$$(\text{for } T=-2.5^{\circ}\text{C} ; 8\times10^{-6}<\dot{\bar{\varepsilon}}<1.3\times10^{-4}\text{s}^{-1}), \quad (6)$$
$$\bar{\varepsilon} > -4.10 \log \dot{\bar{\varepsilon}} - 16.6,$$
$$(\text{for } T=-6^{\circ}\text{C} ; 1\times10^{-6}<\dot{\bar{\varepsilon}}<7\times10^{-5}\text{s}^{-1}), \quad (7)$$
$$\bar{\varepsilon} > -3.50 \log \dot{\bar{\varepsilon}} - 15.6,$$
$$(\text{for } T=-18^{\circ}\text{C} ; 1\times10^{-6}<\dot{\bar{\varepsilon}}<4\times10^{-5}\text{s}^{-1}). \quad (8)$$

As the range from 360~380 kg · m^{-3} represents the average density of naturally settled seasonal snow, it is considered that eqs. (6), (7) and (8) are valid for average snow deposited calmly at -2.5°, -6° and -18°C respectively.

The critical strain curves in Figs. 21 and 22 do not coincide with each other even under

the same condition concerning snow density and temperature. This disaccordance is considered to originate from a difference in structure of snow tested, i. e., drifted snow for the experiments on density dependency and calmly deposited snow for those on temperature dependency, rather than from a difference in snow density, as pointed out previously. A complete description of the fracture condition of snow calls for further research under wider ranges in kinds and structures of snow as well as temperature.

IV. 2. *Tensile Experiment of a Snow Cover on a Slope and Validity of the Fracture Condition*

A snow cover on a slope was subjected to a tensile experiment in the field for examination of the validity of the fracture condition of snow which was obtained in the laboratory with specimens of the limited size. As it was suggested that glide motion of a snow cover on a slope played the principal role in making a tension crack in advance of a ground avalanche release (Endo and Akitaya 1976), artificial glide motion of a snow cover on a slope was generated by the following way.

In autumn of 1980 a short railway was set up on the north slope in the vicinity of the Observatory in parallel to the maximum slope line with an inclination of 17.5°. A four wheel truck with a deck of 1.2 m in length, 0.9 m in width and 0.15 m in height above the ground was placed and anchored at the upslope end of the railway. Four snow catchers (wooden boards 15 cm in height and 90 cm in width) were fixed upright at an equal interval on the deck perpendicularly to the direction of the truck, for securing a snow cover on the deck firmly at its bottom layer, as shown in Fig. 23. When the truck was anchored, a platform was also built and fixed to the slope on the upslope side of the truck. Its surface was on the same plane as the surface of the deck ; its downslope end adjoined the upslope end of the truck and its upslope end was where its surface intersected the surface of the slope ; it had the same width as the truck. So, the side view of the platform was like a wedge tapering upslope. It enabled to smooth out a gap between the surface of the truck and

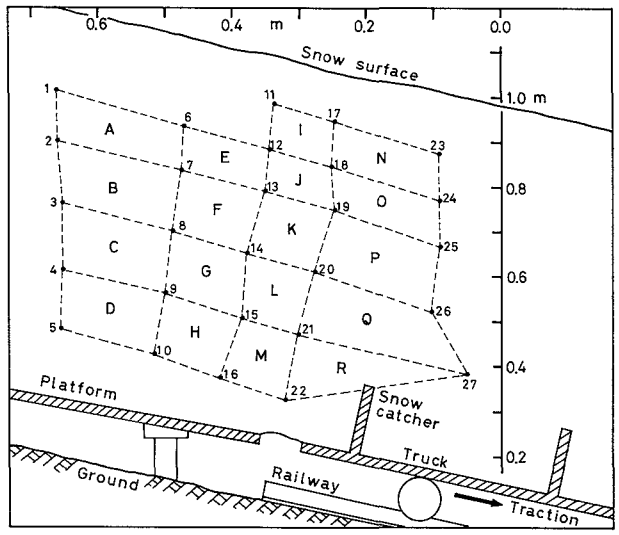

Fig. 23 Schematic diagram of a tensile experiment of a snow cover on a slope, and strain-grids on the lateral sidewall (April 2, 1981, 19 : 00).

that of the slope. After a sufficiently thick snow accumulation covered the slope in the end of winter, snow sorrounding the truck and platform was carefully removed, keeping the exposed snow walls vertical and smooth. Places subjected to snow removal were on both lateral sides of the truck and platform as well as the downslope side of the truck ; the place kept intact was on the upslope side of the platform. As a result, the side walls of the snow cover on the truck and platform were vertical along their outer edges, except for the upslope side of them. Then, a traction device, composed of a motor, a decelerator and a worm-gear jack, was fixed on the ground and connected with the truck through a load cell to measured the resisting force of the snow cover to extension by traction, as shown in Fig. 24.

Twenty-seven markers (thin alminium pins of 1.5 mm in diameter and 15 cm in length) were planted horizontally on a vertical sidewall of the snow cover to be tested referring to the snow stratum making strain grids numbered 1 to 27, as shown in Fig. 23. When released from the anchor, the truck was pulled down along the railway by the traction device, at a constant speed of 6.2 cm · day^{-1}. The coordinates of the 27 markers were precisely measured intermittently to calculate the local strain of the snow cover under test.

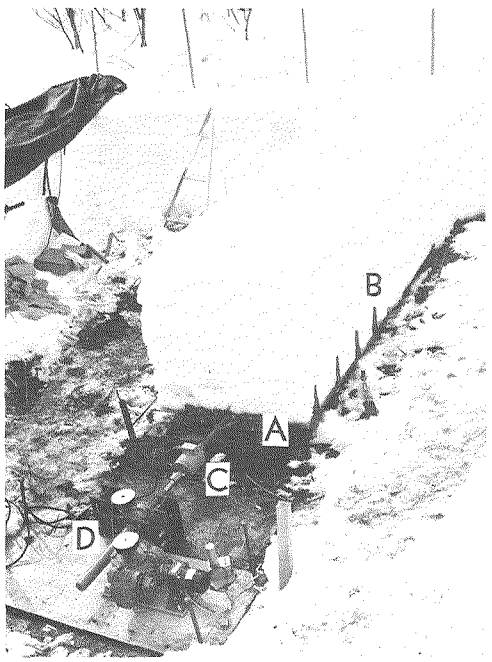

Fig. 24 Tensile experiment of a snow cover on a slope (April 2-4, 1981). A : truck, B : snow catcher, C : load cell, D : traction device.

The local strain of the snow cover was measured on 18 local domains A to R, 17 quadrilaterals and 1 triangles, as shown in Fig. 23. The local strain was calculated by the use of displacements of three neighboring markers under an assumption of homogeneous strain (Jaeger 1956, Shimizu 1968, Shimizu and Huzioka 1975), as Shimizu (1968) clarified experimentally that the homogeneous strain allowed the strain of snow in a unit layer of a snow cover to be sufficiently approximated except for melting snow. For a local domain of a quadrilateral, strain was calculated on two component triangles of the quadrilateral ; then they were averaged. Measurements of the markers' coordinates were made four times through the experiment, i. e., at the start of the experiment (Fig. 23), and 12, 21 and 37 hours after the start. The local strain was calculated taking the final position of a marker in the previous measurement as the initial position for the sucessive measurement. Figures 25 (a), (b) and (c) are graphical expressions of the local strain rate (s^{-1}) in logarithmic

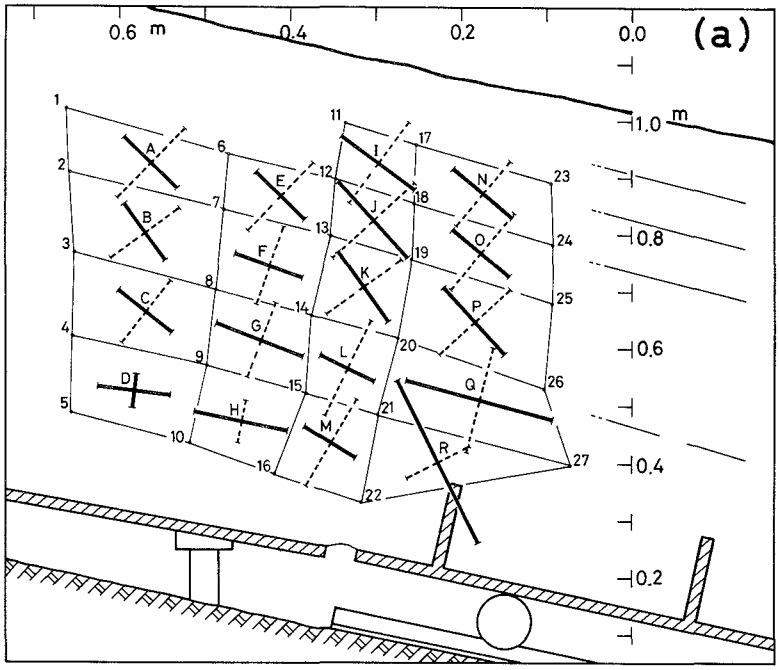
0.6 m
0.4
0.2
0.0
(a)
1.0 m
0.8
0.6
0.4
0.2
A
B
C
D
E
F
G
H
I
J
K
L
M
N
O
P
Q
R

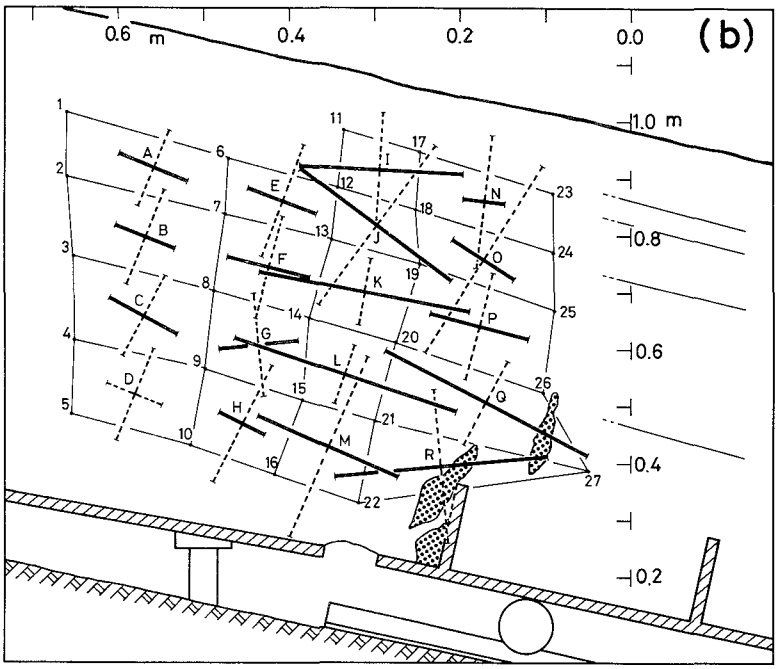
0.6 m
0.4
0.2
0.0
(b)
1.0 m
0.8
0.6
0.4
0.2
A
B
C
D
E
F
G
H
I
J
K
L
M
N
O
P
Q
R

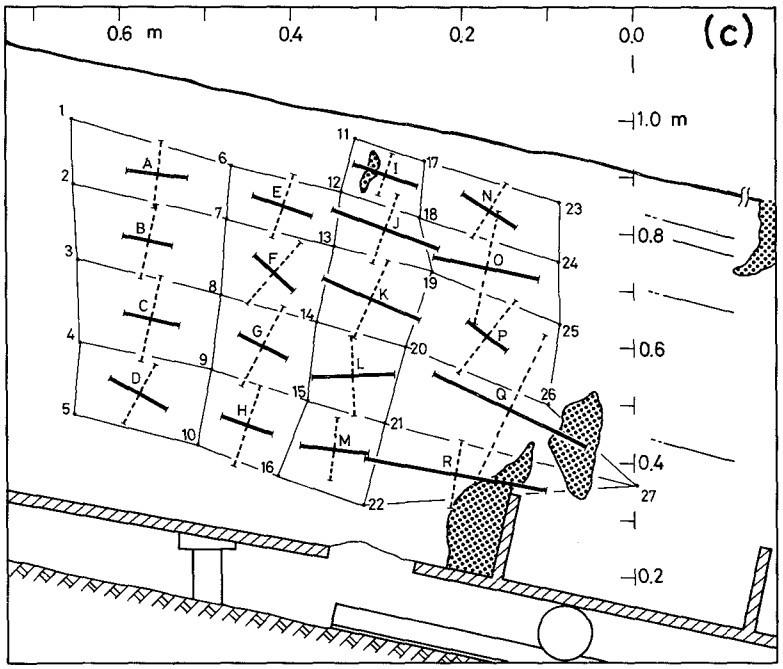

Fig. 25 Distribution of the principal axes of strain and of strain rate (s^{-1}) in local domains on the lateral sidewall of a snow cover on a slope. Strain rate is given by logarithmic value ; a solid line for tension and a broken line for compression.
(a) April 3, 7 : 10, (b) April 3, 16 : 10, (c) April 4, 8 : 00, 1981.

value, and Figs. 26 (a), (b) and (c) are numerical expressions of the local strain (%) and strain rate (s^{-1}) generated in the individual exprimental period.

In the first experimental period for the beginning 12 hours a clear tendency can be seen in Fig. 25 (a) that the orientations of the first principal axes of strain (tensile strain) of the most of local domains were sharply inclined downward in the downslope side. This is a fairly characteristic pattern, compared with those in the stable snow cover on a slope in a tensile region in which most of the first principal axes lay in a position around the horizontal (Huzioka et al. 1978, 1979, 1980). This characteristic pattern of the first principal axes of strain in the snow cover under test must be evidence of exertion of traction on the snow cover in this experimental stage. Moreover, large strain rates of the order of $10^{-6}s^{-1}$ were observed in Q and R, as indicated by a double frame in Fig. 26 (a), while those in all other local domains were of the order of $10^{-7}s^{-1}$ which were merely the common values of those in the stable snow cover on a slope in a tensile region (Huzioka et al. 1978, 1979, 1980). The large values appearing in Q and R are considered to result from a local effect of the traction, as

Q and R were fairly close to the snow catcher of the truck.

As a whole, it can be said in this step that traction of the snow cover under test exerted an influence strongly on the local domains in the vicinity of the action point of the force, but weakly on the further domains.

In the second period between 12 and 21 hours after the start, a large strain rate of the order of $10^{-6}s^{-1}$ appeared in domains I, J, K, L and M, in addition to Q and R, as shown in Figs. 25 (b) and 26 (b), while those of the order of $10^{-7}s^{-1}$ or less in other domains. The first principal axes of strain in the most of domains appeared approximately in parallel to the ground slope in contrast with either those of the first period or of the general case in this area. This is also a fairly characteristic pattern of the local strains, suggesting the mechanical condition in this period under which the tension by the truck was exerted on the entire depth of the snow cover more strongly than in the first period. Furthermore, the right-hand sides of five quadrilateral domains I to M which showed a large strain rate, i. e., the lines of markers 17 to 22, are approximately on the plane perpendicular to the traction, passing through the gap between the fixed platform and the deck of the moving truck. This is considered as an indication that a fracture plane was to be formed along the row of domains I to M. If so, such behavior of the snow cover is fairly similar, in a general view, to those of snow specimens of the limited size in

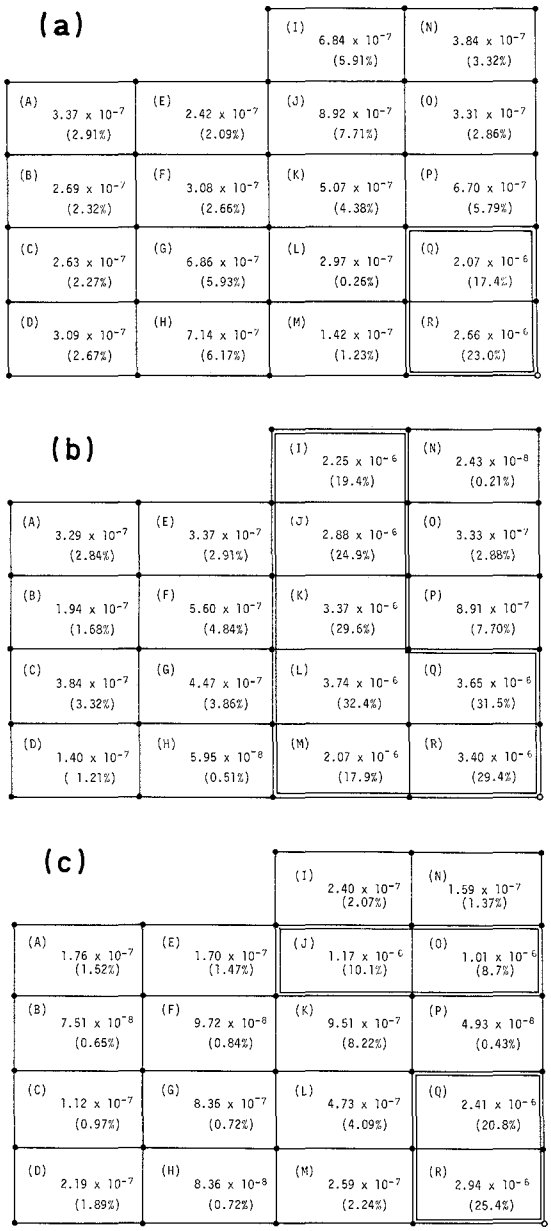

Fig. 26 Distribution of the first principal strain (tension, %) and strain rate (s^{-1}). The double frame indicates a local domain of the snow where the strain and strain rate observed were large. (a) April 3, 7 : 10, (b) April 3, 16 : 10, (c) April 4, 8 : 00, 1981.

the laboratory described previously. Three cracks which appeared in snow in the vicinity of the snow catcher of the truck are likely to have resulted from a strong effect of traction according to their locations.

The final measurement of the experiment, 37 hours after the start, gave large strain rates of the order of $10^{-6}s^{-1}$ in domains J, O, Q and R, and those of the order of $10^{-7}s^{-1}$ or less in all other domains, together with remarkable growth of cracks, as shown in Figs. 25 (c) and 26 (c). On observation of thin sections of snow in the local domains prepared after the experiment, active growth of microcracks was revealed in domains J to M, while no trace of it in A to H.

The following explanation may be given to the behavior of the tested snow cover in this experiment. In the first period of the experiment, tension caused by the traction truck exerted influence strongly on the snow in the vicinity of the snow catcher of the truck, and weakly on those in further locations. In the second period, the tension exerted influence on the entire depth of the snow cover more strongly. A sign of fracture plane appeared as a row of local domains I to M with a large strain rate which was on a plane perpendicular to the tension. Also, large cracks appeared in snow. In the third period, the major part of the traction worked to enlarge the cracks, but not so much as to extend the snow itself.

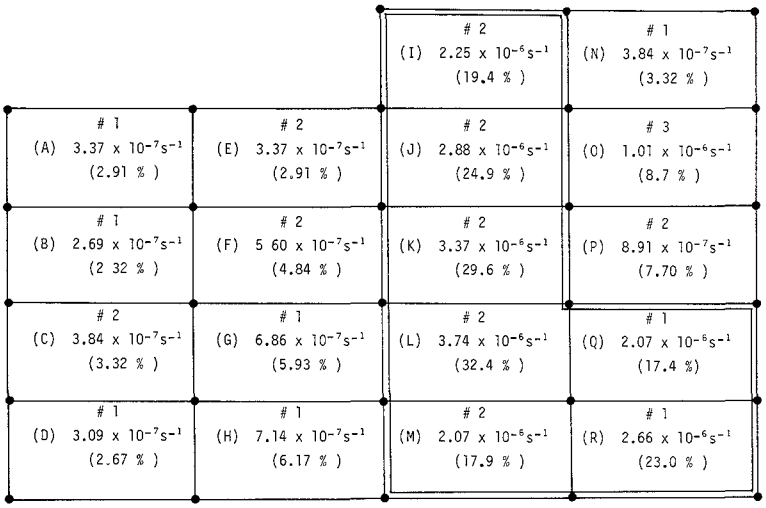

Fig. 27 Distribution of maximums of tensile strain rate (s^{-1}) and strain (%) on the lateral sidewall of a snow cover on a slope ; the values observed after a crack was formed in the local domain were excluded. The number with # given at the top of each frame gives the serial number of the experimental period of the observation. The double frame indicates a local domain where a crack or microcracks were observed in snow, by the final observation. On domains N, O and P, thin sections of snow were not observed.

The largest strain and strain rate in each local domain of the tested snow cover through the experiment were compiled in Fig. 27. When a crack appeared in a domain, the largest values of those up to the previous period were taken. The time of microcrack formation was not detectable in this experiment ; and a sudden change in strain and strain rate did not take place by formation of microcracks. So, the largest values of those through the experiment were used for the domain where microcracks were formed but cracks were not. The domain in which cracks or microcracks were formed was indicated by a double frame in Fig. 27.

As a result the domain in which cracks or microcracks were formed was perfectly coincident with those in which the strain and strain rate observed were large. The difference in numerical values of the strain and strain rate between the fractured and unfractured domains is extremely evident ; i. e., more than 17 % in strain and $2\times10^{-6}s^{-1}$ in strain rate in the fracture domain, while a few percent in strain and of the order of $10^{-7}s^{-1}$ in strain rate in the unfractured domain.

The fracture condition of snow obtained in the previous section was applied to this experimental result for examination of its validity. A snow cover subjected to this experiment was dominantly composed of calmly deposited snow, the snow temperature being 0°C. Thus, as shown in Fig. 28, the data obtained by this experiment were plotted on a diagram of strain rate versus strain together with the critical strain curves of calmly deposited snow

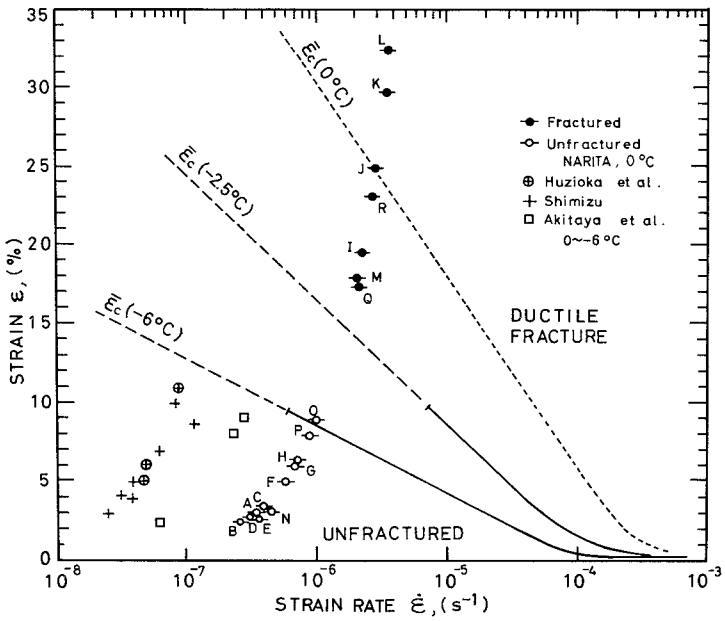

Fig. 28 The fracture condition of snow and field observations.

indicated in Fig. 22. The critical strain curve of snow of 360−380 kg · m^{-3} in density at 0° C (a fine broken line) was drawn by a simple extrapolation of those curves of snow of the same density at −18°, −6° and −2.5°C. In Fig. 28, fractured domains I to M, Q and R appear in a clearly isolated region from the unfractured domains. However, a half of the fractured domains, especially I, M and Q, are evidently not under the fracture condition at 0°C, though all the unfractured domains A to H and N to P are perfectly in the unfractured area of the fracture condition. Here, attention should be paid on the term "the maximum strain/strain rate" in this experiment, as the values were averaged over 10 hours or more of an experimental period, while the real strain/strain rate of snow must have varied with time which had a direct relation to the fracture of snow. It is naturally considered that the real maximum strain/strain rate should be larger than these averaged values. If so, it is likely that the real positions of points I, M, Q and R are closer to the condition than the positions indicated in Fig. 28. Such experimental results support the validity of the fracture condition qualitatively at least, though a quantitative question still remains unsolved.

The results of measurements of internal strain of a snow cover on a slope in the tensile region, obtained by Shimizu (1968), Akitaya et al. (1971) and Huzioka et al. (1971), were also plotted in Fig. 28. All these measurements were made on the stable snow cover without cracks or microcracks in it at 0°~−6°C. As seen clearly in the diagram, all the measurements of the previous researchers lie in the unfractured region. This fact also supports the validity of the fracture condition. It is imperative that the present description of the fracture condition of snow will be brought to completion by further research, changing the parameters over wider ranges.

V. Rheological Interpretation of Fracture of Snow

Generally, a rheological model can be a great help in explaining the mechanical property of snow, though it may be necessary to apply different models on a case by case basis. De Quervain (1946), Yosida (1953) and Kojima (1954) adopted Burger's model for investigation of behavior of snow under stress, which was a combination of a Maxwell and a Voigt model connected in series. Salm (1971) opted for a nonlinear rheological model to derive his failure criterion of snow. Meanwhile, Kinosita (1957) showed that the outline of behavior of snow under stress can be described well even only by the Maxwell model. For simplicity's sake the author draws now on the Maxwell model (Fig. 29) to make a brief rheological interpretation on fracture of snow under tensile stress.

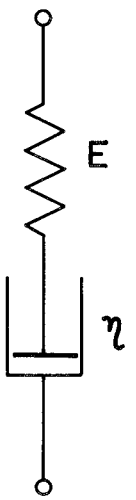

Fig. 29
Maxwell model

Reiner and Weissenberg (1949) pointed out the followings. Namely, total deformation of a solid body is generally composed of elastic deformation and viscous deformation ; total work W to deform the solid body

is consumed to achieve these two kinds of deformation properly ; then, the work done for elastic deformation, W_E, is charged in the body as potential energy, whereas the work done for viscous deformation, $W\eta$, is dissipated thermally. Then,

$$W = W_E + W\eta. \tag{9}$$

When the charged energy in the body, W_E, exceeds a certain critical value W_0, the body is broken up. That is, the fracture condition of a solid body under stress is given as,

$$W - W\eta = W_E \geq W_0. \tag{10}$$

This equation suggests that fracture of a solid body under tensile stress corresponds to breaking up of the spring element of the Maxwell model.

Generally, the behavior of a solid body under stress varies according to the balance between the elastic deformation energy W_E of the spring, and the viscous deformation energy $W\eta$ of the dashpot of the corresponding Maxwell model.

i) If $W_E \ll W\eta$, the dashpot is hardly deformed, while the spring is deformed elastically and attains to the critical extension easily, then breaks up. Such behavior of the Maxwell model corresponds to brittle fracture of snow defined by type a.

ii) If $W_E \gg W\eta$, the spring is hardly deformed, while the dashpot is deformed viscously. This corresponds to viscous deformation of a body or creep of snow defined by type d.

Namely, for brittle fracture,

$$\frac{W_E}{W_\eta} = \frac{\int E \cdot \varepsilon_E \, dt}{\int \eta \cdot \varepsilon_\eta \, dt} = \frac{E \cdot \varepsilon_E \, T}{\eta \cdot \varepsilon_\eta} \ll 1, \tag{11}$$

and for creep,

$$\frac{W_E}{W_\eta} = \frac{E \cdot \varepsilon_E \, t}{\eta \cdot \varepsilon_\eta} \gg 1, \tag{12}$$

where W_E : deformation energy of the spring in a Maxwell model,

$W\eta$: deformation energy of the dashpot of the model,

E : elastic modulus of the spring element,

η : viscosity coefficient of the dashpot,

ε_E : strain of the spring element,

ε_η : strain of the dashpot,

t : working time of force.

The relaxation time τ of a Maxwell model is given as,

$$\tau = \eta / E, \tag{13}$$

and then,

$$t/\tau = \varepsilon_\eta / \varepsilon_E \tag{14}$$

This is the fracture condition of a Maxwell model, where t is the working time of force necessary to break up the spring element. If $t<\tau$, the model will be broken up as ε_E attains to a critical value, and if $t>\tau$ on the contrary, the model will be deformed viscously without fracture.

The lower limit of the brittle fracture of snow was investigated by the use of the previous experimental result. To estimate the relaxation time of snow it is secessary to obtain experimentally the viscosity coefficient η and the elastic modulus E of the snow.

The viscosity coefficient η can be estimated from the stress-strain rate curve of the

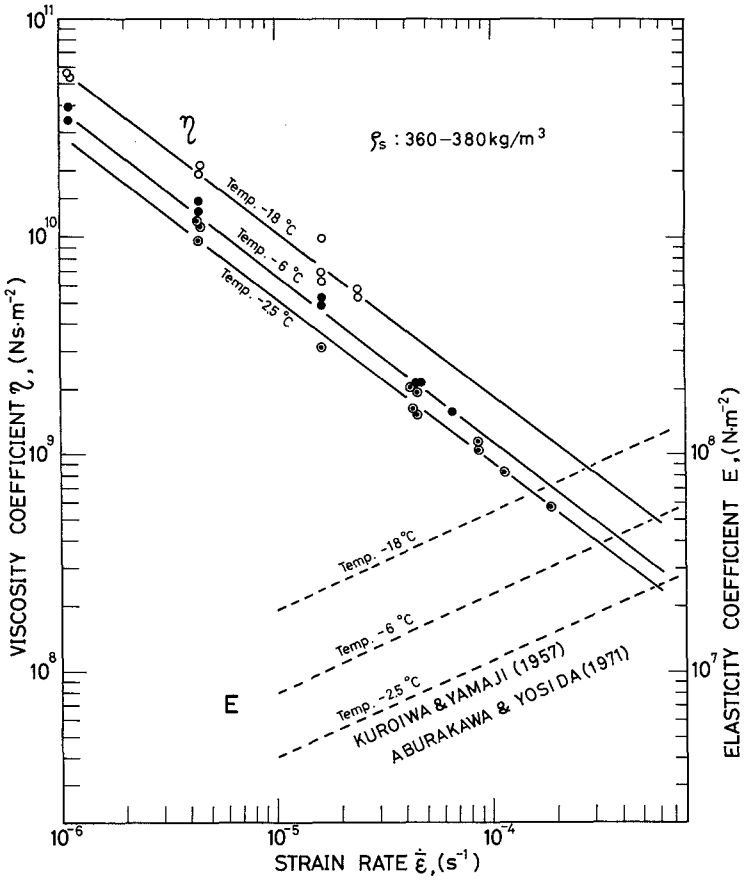

Fig. 30 Viscosity coefficient η (Ns·m^{-2}) and elastic modulus E (N·m^{-2}) of snow.

snow. Visco-elastic equation of a Maxwell model is given as,

$$\frac{d\varepsilon}{dt}=\frac{1}{E}\left(\frac{dF}{dt}\right)+\frac{1}{\eta}F. \tag{15}$$

If the body is deformed viscously, the first term of the right side of eq. (15) vanishes ; and the viscosity coefficient η of the body is calculated as,

$$\eta=F/\dot{\varepsilon}. \tag{16}$$

A number of cases of $dF/dt=0$ were found in the experiments mentioned earlier in this paper, whereby the values of viscosity coefficient η (Ns · m^{-2}) of snow of 360~380 kg · m^{-3} in density were calculated for each case. They were plotted in an $\dot{\varepsilon}-\eta$ diagram, as shown by solid lines in Fig. 30. For the case of brittle fracture, this method cannot be applied to obtain the viscosity coefficient of snow, as it lacks a viscous deformation process. So, the solid lines of η in Fig. 30 were simply extended into the brittle fracture region of the order of 10^{-4}s^{-1} in the strain rate range.

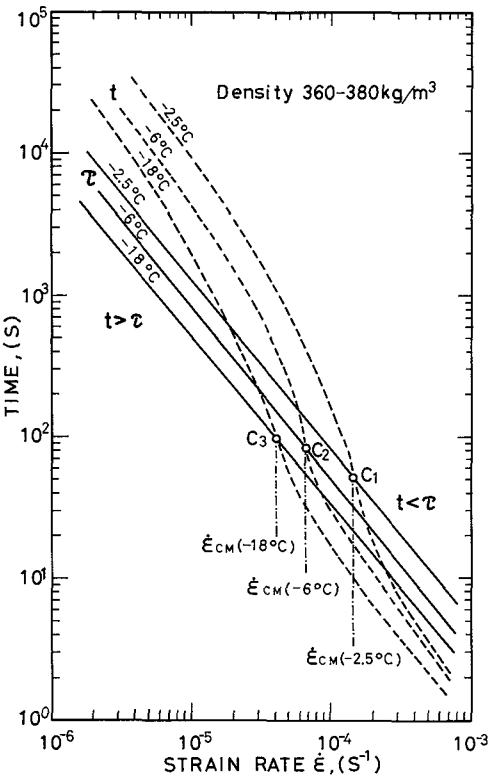

Fig. 31 The lower limit of brittle fracture of snow. C : intersection of t- and τ-curves ; $\dot{\varepsilon}_{CM}$: critical strain rate of Maxwell model for transition from fracture range to viscous deformation range.

The real elastic range of snow is so small, less than 0.1 % in strain, that it is practically difficult to estimate the elastic modulus E from the stress-strain curve of snow. Then, the values of E obtained previously by the following researchers using dynamic methods were used in this paper : Kuroiwa and Yamaji's value (1957) obtained by the oscillation method of a snow bar with a frequency of 200~380 Hz, and Aburakawa and Yosida's value (1971) by a double-pendulum method with a frequency of 2 Hz. From their results, values of η of fine-grained old snow of around 370 kg · m^{-3} in density were plotted in an $\dot{\varepsilon}-E$ diagram as shown by broken lines in Fig. 30.

By the use of these values of η and E, the values of the relaxation time τ of snow of 360~380 kg · m^{-3} in density were calculated by eq. (13). The working time t necessary to break up a snow specimen, in brittle fracture or in formation of microcracks in snow, was estimated

from the resisting force-strain curve of the experiments. From these results, the relaxation time curve (τ-curve in solid lines) and the working time curve (t-curve in broken lines) both at $-2.5°$, $-6°$ and $-18°C$, were obtained, as shown in Fig. 31.

As clearly seen on the diagram, the $t-$curve interesects the corresponding $\tau-$curve in the same way, at a certain strain rate $\dot{\varepsilon}_{CM}$ at the same temperatures. The Maxwell model is broken up when the strain attains to a certain critical value, in the right side region of the intersection C as $t<\tau$ there. On the other hand, in the left side region of C it is not possible to measure experimentally the working time t necessary to break up the Maxwell model, because $t>\tau$ there, and the Maxwell model is not broken up in any way but it is deformed viscously. As a matter of fact, however, the working time t necessary to make a local minute fracture such as formation of microcracks of type b and type c was experimentally measured. The Maxwell model is definitely inapplicable to such behavior of snow as formation of the microcracks in snow, which shows limitation in applicability of the Maxwell model.

Meanwhile, it was found that the critical strain rate $\dot{\bar{\varepsilon}}_C$ of real snow for transition from brittle fracture (type a) to ductile fracture (type b), given in Fig. 19, coincided considerably well with the critical strain rate $\dot{\varepsilon}_{CM}$ for transition from the fracture region to the creep region of the Maxwell model at different temperatures ; that is, at $-2.5°$, $-6°$, $-18°C$, respectively for $\dot{\bar{\varepsilon}}_C=1.6\times10^{-4}$, 6.8×10^{-5}, $4.4\times10^{-5}s^{-1}$; $\dot{\varepsilon}_{CM}=1.3\times10^{-4}$, 6.5×10^{-5}, $4.0\times10^{-5}s^{-1}$. Such a close coincidence of the values of $\dot{\bar{\varepsilon}}_C$ and $\dot{\varepsilon}_{CM}$ is a point of great interest, calling for a further research for clarification of it.

VI. Concluding Remarks

Snow specimens were subjected to tensile experiments in the laboratory and field. First, according to strain rates, the four general types were introduced in classification of the deformation and fracture of snow under tensile stress. They are types a (brittle fracture), b and c (two modes of ductile fracture) and d (viscous deformation), which corresponded to the strain rates of the order of $10^{-4}s^{-1}$ or more ; $10^{-5}\sim10^{-4}s^{-1}$; $10^{-6}\sim10^{-5}s^{-1}$; $10^{-7}s^{-1}$ or less, respectively. Then upon investigations made concerning the density dependency and the temperature dependency of the foregoing types as well as the formation of deformation or fracture, it was found that the boundary between the two adjacent types shifted toward the side of larger strain rates with increasing snow density and rising temperature. The critical strain rate $\dot{\bar{\varepsilon}}_C$ for transition from brittle to ductile fracture appeared in the vicinity of the maximum strength of snow, which increased with increasing snow density and lowering temperature. For defining the fracture of snow by the formation of microcracks, the fracture condition of fine-grained old snow was given using $\dot{\bar{\varepsilon}}_C$.

Meanwhile, the result of a tensile experiment of a snow cover on a slope in the field supported the validity of the foregoing fracture condition, though not all the quantitative

questions were solved. For acquiring a thorough knowledge of the fracture condition we are called on to continue a research by varying control fractors widely, especially the kinds and structures of snow.

Finally, a rheological interpretation was briefly made, using the Maxwell model, which was capable of giving a satisfactory explanation to the behavior of snow of types a and d, but not the behavior of types b and c. As the most interesting point, however, a good coincidence was found between the numerical values of the critical strain rate $\dot{\varepsilon}_{CM}$ of the Maxwell model for transition from the fracturing range to the viscous deformation range and those of $\dot{\bar{\varepsilon}}_C$ of snow for transition from brittle to ductile fracture. A further look into this point is called for in reaching a clearer understanding of the nature of tensile fracture of snow.

Acknowledgements

The research was carried out at the Avalanche Observatory, located in Toikanbetsu in northern Hokkaido, Japan, of the Institute of Low Temperature Science, Hokkaido University, and in the vicinity of the Observatory. The author would like to express his gratitude to Dr. T. Huzioka, Dr. S. Kinosita, Dr. H. Shimizu and Dr. E. Akitaya for encouragement and valuable advice in the preparation of this paper, together with to Dr. S. Takikawa for his kindness, offering convenience of the work at Toikanbetsu.

The author is also indebeted to Mr. M. Himori and Mr. K. Shinbori, members of workshop of the Institute for making the instruments for the work.

References

Aburakawa, H. and Yosida, Z. 1971 A double pendulum used for the determination of low frequency Young's modulus of snow and ice. *Low Tomp. Sci., Ser. A,* **29,** 37-49.

Akitaya, E. 1974 Statistics of avalanche accidents in Japan (1918-1974)—by the use of hand-sorting edgepunched cards—. *Seppyo,* **36,** 6-13.

Akitaya, E. and Kawada, K. 1971 Studies of the behavior of a snow cover on a mountain slope II. —displacements, strains, glides—. *Low Temp. Sci., Ser. A,* **29,** 135-149.

De Quervain, M. 1946 Kristallplactische Vorgange in Schee-aggregate. II. Mitteilungen aus dem eidg. Institut für Schnee-und Lawinenforschung.

Endo, Y. and Kkitaya, E. 1976 Studies of the behavior of a snow cover on mountain slope VI. Formation and mechanism of bump-shaped undulation. *Low Temp. Sci., Ser. A,* **34,** 99-110.

Huzioka, T., Shimizu, H., Akitaya, E., Narita, H., and Kawada, K. 1971 Studies of the behavior of a snow cover on mountain slope I. —strains and strain rates—. *Low Temp. Sci., Ser. A,* **29,** 125-134.

Huzioka, T., Shimizu, H., Akitaya E., Narita, H., Kawada, K., Izumi, K., Okano, T. and Takemori, S. 1978 Strain rates and stresses of snow on a mountain slope, Toikanbetsu Northern Hokkaido I. *Low Temp. Sci., Ser. A,* **36-37,** *Data Rep.,* 39-69.

Huzioka, T., Shimizu, H., Akitaya, E., Narita, H. and Okano, T. 1979 Strain rates and stresses of snow on a moutain slope, Toikanbetsu, Northern Hokkaido. II. *Low Temp. Sci., Ser. A,*

38, *Data Rep.,* 33-37.
Huzioka, T., Shimizu, H., Akitaya, E. and Narita, H. 1980 Strain rates and stresses of snow on a mountain slope, Toikanbetsu, Northern Hokkaido. III. *Low Temp. Sci., Ser. A,* **39,** *Data Rep.,* 13-33.
Ikarashi, T. 1979 The frequency of avalanche release in Niigata prefecture. *Rep. Natl. Res. Center Disaster Prev.,* **21,** 89-102.
Jaeger, J. C. 1964 Elasticity, Fracture and Flow, Methuen & Co. London, 22-33.
Japanese Society of Snow and Ice. 1964 The classification of avalanche. *Seppyo,* **26,** 195-198.
Keeler, C. M. 1969 Some mechanical properties of alpine snow. *CRREL Res. Rep.* **271.**
Keeler, C. M. and Weeks, W. F. 1967 Some mechanical properties of alpine snow, Montana 1964-66. *CRREL Res. Rep.* **227.**
Kinosita, S. 1957 The relation between the deformation velocity of snow and two types of its deformation (plastic and destructive.). *Low Temp. Sci., Ser. A,* **16,** 139-166.
Kojima, K. 1954 Visco-elastic property of snow. *Low Temp. Sci., Ser. A,* **12,** 1-13.
Kuroiwa, D. and Yamaji, K. 1956 Study of elastic and viscous properties of snow by the vibration method II. *Low Temp. Sci., Ser. A,* **15,** 43-58.
Martinelli, M. Jr. 1971 Physical properties of alpine snow related to weather and avalanche conditions. Forest Service Research Paper RM-64, U. S. Dept. of Agriculture.
McGabe, S. L. and Smith, F. W. 1978 A mechanical test procedure for avalanche snow. *J. Glaciol.* **20.** 433-438.
Narita, H. and Shimizu, H. 1974 Distribution of snow avalanches in the avalanche station area, Toikanbetsu, Northern Hokkaido, I. *Low Temp. Sci., Ser. A,* **32.** *Data Report,* 40-54.
Narita, H. and Shimizu, H. 1975 Distribution of snow avalanches in the avalanche station area, Toikanbetsu, Northern Hokkaido. II. *Low Temp. Sci., Ser. A,* **33.** *Data Report,* 35-46.
Narita, H. and Shimizu, H. 1976 Distribution of snow avalanches in the avalanche station area, Toikanbetsu, Northern Hokkaido. III. *Low Temp. Sci., Ser. A,* **34.** *Data Report,* 27-38.
Narita, H. and Shimizu, H. 1977 Distribution of snow avalanches in the avalanche station area, Toikanbetsu, Northern Hokkaido. IV. *Low Temp. Sci., Ser. A,* **35.** *Data Report,* 35-44.
Narita, H. 1980 Mechanical behavior and structure of snow under uniaxial tensile stress. *J. Glaciol.* **26,** 275-282.
Perla, R. I. and Martinelli, M. Jr. 1976 Avalanche handbook. Agriculture handbook 489, Forest Service, U. S. Dept. of Agriculture.
Reiner, M. 1949 Deformation and Flow. H. K. Lewis & Co., 346 pp.
Salm, B. 1971 On the rheological behavior of snow under high stresses. *Contr. from Inst. Low Temp. Sci.,* No. 23, 43pp.
Shimizu, H. 1968 Study on internal strain of snow cover on slope I. *Low Temp. Sci., Ser. A,* **26,** 143-168.
Shimizu, H. and Huzioka, T. 1975 Internal strains and stresses of snow cover on slopes. Proceedings of the International Symposium on Snow Mechanics, Grindelwald, 1974. The International Association of Hydrological Science, Publication No. 114, 321-331.
Shinojima K. 1962 Study of the visco-elastic deformation of deposited snow. Railway Tech. Res. Rept., No. 328, The Railway Tech. Res Inst., Japanese National Railways, 1-56.
Shoda, M. 1967 Areal observations and thin section studies on avalanches (Avalanche studies during 1962-1966 in Shiozawa). *In* Prysics of Snow and Ice, (H. Oura, ed.), Inst. Low Temp. Sci., Part 2, 1137-1149.
Sommerfeld, R. A. 1971 The relationship between density and tensile strength in snow. *J. Glaciol.* **10,** 357-362.
Yosida, Z. 1953 Visco-elastic property and break-down resistance of snow. *Low Temp. Sci.,* **10,** 1-11.